MINERALOGICAL ZONING OF THE PGE-Cu-Ni OREBODIES AT THE CENTRAL PART OF OKTYABR'SKY DEPOSIT, NORILSK DISTRICT, RUSSIA

Tolstykh N.D.[1], Krivolutskaya N.A.[2], Kanhimbue L.S.[3], Gongalsky B.I.[4], Kuz'min I.A.[1]

[1] *VS Sobolev Institute of Geology and Mineralogy, SB RAS, Novosibirsk*

[2] *VI Vernadsky Institute of Geochemistry and Analytical Chemistry, RAS, Moscow*

[3]*Empress Catherine II Saint Petersburg Mining University, St. Petersburg*

[4]*Institute of Geology of Ore Deposits, Petrography, Mineralogy and Geochemistry, RAS, Moscow*

Abstract. Mineralogical features of two orebodies or lenses (C-3 and C-4) at the central part of the Oktyabr'sky deposit were identified. Multidirectional mineralogical zoning in the northern and southern orebodies is shown, confirming the hypothesis of their formation from various magmatic flows, which have individual features and their own modes of formation. The southern C-3 and northern C-4 orebodies differ in their mineralogical associations: the first one is characterized by a high-sulfur association of sulfides, and the second one contains minerals with a sulfur deficit (talnakhite, sugakiite). Variations in Fe and Ni ratios in pentlandite are controlled by the volatility of sulfur during ore crystallization. Direct crystallization zoning is observed in the disseminated ores of the C-4 orebody (borehole RT-107), where the fugacity of sulfur (fS2) increases from bottom to top. Whereas in orebody C-3 (borehole RT-30) fS2 decreases in the same direction. The identified reverse zoning coincides with the vectors of the evolution of ore systems in various blocks of the Main Ore Body (MOB) of the Oktyabr'sky deposit. The difference in typomorphic features of disseminated ores of the southern and northern orebodies is confirmed by differences in the associations of platinum group element minerals (PGMs). Disseminated ores in picritic gabbro-dolerites and massive pyrrhotite ores in the exocontact of the intrusion within the southern orebody differ in the specialization of PGMs: the first is characterized by minerals of the Pd-Bi-Sb-Te system, the latter - only Pt minerals. The similarity of these types of ores lies in the similar reverse mineralogical and geochemical zoning from top to bottom along the sections, caused by the evolution of the sulfide melt in this direction. The formation of reverse zoning of disseminated ores (zones of "marginal reversion") is probably due to the action of the mechanism of repeated influx of a melt of an increasingly primitive composition into the upper parts of the crystallizing

This is a 'preproof' accepted article for Mineralogical Magazine. This version may be subject to change during the production process.
DOI: 10.1180/mgm.2024.20

flow. Unidirectional trends in massive and disseminated ores are more likely due to the action of the same type of mechanism.

Keywords: PGE-Cu-Ni ore; geochemistry-mineralogical zoning; evolution of sulfide melt; northern and southern orebodies; Oktyabr'sky deposit

1. INTRODUCTION.

The Oktyabr'sky deposit plays an important role in solving of the genetic problems of the unique platinum-copper-nickel ores at the Norilsk region, and it is the largest deposit related to the Kharaelakh layered intrusion which is localized in the south of the Kharaelakh trough (Fig. 1).

The Oktyabr'sky deposit is a collection of at least 15 massive (and overlying disseminated) ore bodies or lenses (Dyuzhikov et al., 1992; Stekhin, 1994; Torgashin, 1994). They can be located close to each other or be spatially separated as the C-3 and C-4 ore bodies. All these ore bodies (or lenses) as a whole make up the Oktyabr'sky deposit. A huge amount of analytical data were obtained for the MOB - lode of massive sulfide ore (4 x 2 км), and thickness up to 50 m. The genesis of the MOB has been the subject of intensive discussions for several decades (Genkin, 1968; Dodin and Batuev 1971; Distler et al., 1975, 1988, 1996; Genkin et al., 1981; Zientek and Likhachev, 1992; Likhachev, 1994, 2006; Naldrett et al., 1994, 1995, 1996; Naldrett, 2004; Sluzhenikin, 2011; Krivolutskaya et al., 2018, and many others).

The MOB has mineralogical zoning: mooihoekite ($Cu_9Fe_9S_{16}$) – talnakhite ($Cu_{18}(Fe, Ni)_{18}S_{32}$) – chalcopyrite ($CuFeS_2$) ore transform into cubanite ($CuFe_2S_3$) ore, and then into pyrrhotite ($Fe_{1-x}S$) ore from center to flank (Dyuzhikov et al., 1992; Torgashhin, 1994; Lul'ko et al., 1994; Naldrett et al., 1995; Valetov et al., 2000; Gorbachev, 2006; Dodin et al., 2009). That is, the iron content in ores increases in this direction. The origin of this «reverse» zoning is one of the main genetic questions. MOB cannot be considered as a single lode crystallized in a closed system, since from the point of view of crystallization differentiation the more fractionated parts of ore bodies enriched in Cu, platinum group elements (PGE) incompatible with monosulfide solid solution (Mss) should be located on the periphery (Distler et al., 1975; Zientek et al., 1994; Barnes et al., 2011). Experimental (Likhachev and Kukoev, 1973; Sinyakova et al., 2019) and modeling (Distler, 1975; Kalugin and Latypov, 2009) work confirm that direct zoning is formed during fractional crystallization when more fractionated constituents of sulfide melts are distilled to the periphery.

The horizontal zoning of the Oktyabr'sky deposit is very complex, and reflects the interaction of different-scale genetic factors: the separation of the sulfide melt in the intermediate chamber into Fe-rich and Cu-rich fractions that can be introduction separately (Gorbachev and

https://doi.org/10.1180/mgm.2024.20 Published online by Cambridge University Press

Nekrasov, 2004; Gorbachev, 2006; Likhachev, 2006); various directions of the flows (streams) of sulfide melts and the pattern of these flows in laterally (Stekhin, 1994); single-act or the pulsating nature of their introduction; the fractionation of the sulfide melt during the flow differentiation with the distillation of its more cuprous derivatives into the frontal parts.

The vertical zoning of ore bodies depend on: the degree of fractionation of the sulfide melt in situ and the behavior of elements compatible and incompatible with Mss during its crystallization; possible degassing of the sulfide melt (Godlevsky, 1968; Gorbachev, 2006) when surface capillary forces dominant over gravity (Barnes et al., 2019); the pulsation mode of incoming melts (Latypov et al., 2007, 2011; Egorova and Latypov, 2013).

If we consider the Oktyabr'sky deposit on a large-scale, that the influence of the Norilsk-Kharaelakh fault is important for the overall configuration of ore zoning (Stekhin, 1994). The zoning of ores is associated primarily with the action of a series of linear flows directed from the fault and being supply channels for intrusive material (Fig. 2). Each flow is characterized by the distribution of pyrrhotite ores in the root parts and near the fault, and more cuprous ores forming halos around the pyrrhotite ores (Kunilov, 1994). The MOB is composed of at least two ore lenses corresponding to the different flows of sulfide melt: pyrrhotite is predominant in the first lens, and mooihoekite-cubanite-chalcopyrite assemblage is common in the second lens (Torgashin, 1994; Kalugin and Latypov, 2010, 2012). The vertical zoning of cuprous and pyrrhotite ores are directly opposite: the contents of Cu, PGE and Au increase from the bottom to the top (direct zoning) in cuprous lenses, while these elements increase from the top to the bottom in pyrrhotite lenses – reverse zoning (Fig. 3) (Torgashin, 1994; Gorbachev, 2006; Kalugin and Latypov, 2010, 2012).

Lenses C-3 and C-4 belong to different flows of silicate magma and sulfide melt (Fig. 2): northern lens C-4 belongs to a branch of the extended «Oktyabr'sky flow», and southern lens C-3 belongs to another flow (unnamed), extending northwest from the regional fault (Stekhin, 1994). Their study is very important for understanding the conditions for the formation of the deposit as a whole (Krivolutskaya, 2014; Krivolutskaya et al., 2019; 2021).

We present new mineralogical data on two ore bodies in the central part of the Oktyabr'sky deposit, including both massive and disseminated ores located at the bottom of the Kharaelakh intrusion: C-3 in the south and C-4 in the north of this area (Fig. 2). These boreholes are characterized by different mineral associations of both sulfides and platinum group minerals (PGM). This work has two goals: i) to demonstrate the mineralogical differences and similarity between disseminated and massive ores; ii) to show typomorphic features of disseminated ores in picritic gabbro-dolerite over C-3 (RT-30 borehole) and C-4 (RT-107 borehole) orebodies to verify the difference in their genesis.

2. BRIEF GEOLOGY OF THE NORILSK DISTRICT

https://doi.org/10.1180/mgm.2024.20 Published online by Cambridge University Press

The geology of the Talnakh ore cluster and the Oktyabr'sky deposit, related to the Kharaelakh intrusion is described in many publications (Zolotukhin, 1964; Zolotukhin et al., 1975; Dyuzhikov et al., 1992; Torgashin, 1994; Stekhin, 1994; Likhachev, 1996; Turovtsev, 2002, and many others). This intrusion belongs to the Noril'sk intrusive complex (Dyuzhikov et al., 1992) and is located within the carbonate-sulfate-terrigenous, mostly, at the boundary of the Razvedochninsky and Kureysky Formations, and partially in the Manturovsky Formation (western flanks). The Devonian sediments are overlapped by the coal-bearing Tunguska series and P_3-T_1 tuff-lavas of the Ivakinsky, Syverminsky, Gudchikhinsky, Khakanchansky, Nadezhdinsky, Morongovsky, and Mokulaevsky formations (Fig. 1, 4). The Kharaelakh intrusion, like other intrusions of the Noril'sk complex, is composed of a differentiated series of gabbro-dolerites, with varying amounts of olivine which decreases from bottom to top (Fig. 4), i.e., contact, taxitic, picritic, olivine, olivine-bearing, olivine-free; leucogabbro, gabbro-diorite, ferrogabbro, upper taxitic and upper picritic gabbro-dolerites form upper intrusive zone. Hereinafter, the nomenclature of rocks adopted in the legend to the Geological Map of a scale of 1: 200,000 is used (Geological Map.., 1994).

The picritic gabbro-dolerite are considered cumulative part of the main layered series (Likhachev, 1996; Distler et al., 1999). Massive ores of various thicknesses are located at the contact of the intrusion with the host-rocks. They are separated from the intrusion by a horizon of host hornfelses, for example, which reach 19 m in RT-30 borehole and only 3 m in RT-107 (Fig. 5).

3. METHODS OF ANALYSIS

The analyses of sulfides and minerals of the platinum group elements (PGM) and high-resolution electronic imaging were performed at the Analytical Center for Multi-Element and Isotope Research of the IGM of SB RAS, Novosibirsk (N.S. Karmanov) by X-ray spectral methods on microanalyzers (SEM-EDS) MIRA 3 LMU (Tescan Ltd) with an INCA Energy 450+ XMax 50+ and Inca Wave 500 microanalysis system (Oxford Instruments Ltd). Probe size ~2 μm, accelerating voltage 20 kV; probe current 30–50 nA over the sample surface; probe diameter ~1 μm. The measurement duration is 20 seconds for each analytical line. The following standards were used: FeS_2 (S), $PtAs_2$ (As), HgTe (Te), metallic Zn, Co, Ni, Cu, Pt, Pd, Au, Ag, Sn, Sb, etc. The limit of detection for the most elements was 0.2–0.3 % (3 sigma criterion). The correction of matrix effects is performed using the software XPP algorithm. The accuracy and reproducibility of the analytical procedure were evaluated by comparing the analyses of EDS and WDS methods of sulfides (pyrrhotte, pentlandite, and chalcopyrite) in the RT-107 borehole, which showed the identity of the analyses for macrocomponents (Fe, Ni, Cu, Co), which is also confirmed by special tests (Korolyuk et al., 2009). We also carried out a comparison of EDS and WDS analyzes of

https://doi.org/10.1180/mgm.2024.20 Published online by Cambridge University Press

pentlandite from all samples of picritic gabbro-dolerites in both boreholes. We were convinced of the identity of the compositions of pentlandite obtained by different methods. EDS results were used since all other minerals were analyzed by X-ray spectral methods on microanalyzers (SEM-EDS) MIRA 3 LMU.

3. RESULTS

3.1. General characteristics of the sulfide ores

Sulfide associations and PGMs were studied in samples of disseminated ores from picritic and taxitic gabbro-dolerites above the northern body C-4 and southern body C-3 (in boreholes RT-107 and RT-30, correspondingly). Picritic gabbro-dolerites of the Oktyabr'sky deposit, as well as all other deposits of the Norilsk complex, are represented by fine-medium-grained massive rocks consisting of (wt.%): olivine (50-80), clinopyroxene (20-30), plagioclase (20-40), and orthopyroxene (about 5). Sulfides in the picritic gabbro-dolerite of both boreholes are composed of drops and small segregations of chalcopyrite-pentlandite-cubanite-pyrrhotite composition (Fig. 6 a-d). Massive ores of southern C-3 orebody are essentially pyrrhotite composition. Pyrrhotite often occurs as intergrowths of crystals of various modifications (troilite and hexagonal), as well as exsolution inclusions of pentlandite of second generations in pyrrhotite (Fig. 6 h). Chalcopyrite grains of various sizes are surrounded by pentlandite rims of the 1-st generation (Fig. 6 h, i).

The sulfur concentration in the disseminated ores in the picritic gabbro-dolerite does not exceed 6 wt.%, and 0.5 wt.% in taxitic rocks. PGE contents in both varieties are the units of percent; Pd prevails over Pt. The sulfur concentration in massive ore varies between 41.8–47.8 wt. % and the (Pd+Pd) concentrations reach 30 ppm.

3.2. Sulfide associations.

We have analyzed disseminated sulfides in the folowing samples taken from different levels of the picritic gabbro-dolerites, i.e., in RT-30: 1501.2, 1516, 1523 and 1527 meters, and in RT-107: 1652, 1657.2 and 1665.4 meters (Fig. 5). They are composed mainly of pyrrhotite (Po) or troilite (Tr), chalcopyrite (Ccp), and pentlandite (Pn) (Table 1).

Iron-nickel ratio in pentlandite varies significantly in the picritic gabbro-dolerite in the sections: both ferruginous and nickel-rich varieties are present but Fe-rich pentlandite predominates (Fig. 7 a,b). It contains Co up to 3.47 wt.% (Table 1). The most Fe-rich compositions of pentlandite occur et a deeper horizon (1665.4 m) of picritic ore over the northern orebody C-4, and the content of Ni in pentlandite, as well as S in pyrrhotite, increase up the section toward the horizon of 1652 m (Table 1, Fig. 7 a). Whereas the opposite direction of these changes occurs in the disseminated ore over the southern orebody: Fe-rich Po and S-poor Po (troilite) are located in

https://doi.org/10.1180/mgm.2024.20 Published online by Cambridge University Press

the upper part of the picritic layer (1501.2 m), and the most enriched in nickel – at a depth (1527 m) (Table 1, Fig. 7 b).

A very important diffference between the northern and southern disseminated ores is: the first ones (in borehole RT-107) contain sugakiite $Cu(Fe,Ni)_8S_8$ (Fig. 7 a) and sulphides deficient in sulfur of the chalcopyrite group (approaching in composition to talnakhite) (Fig. 7 d), while the second ores (RT-30) comprise only stekhiometric chalcopyrite (tetragonal). Sugakiite, a rare mineral, occur as granular (60-120 μm) grains intergrown with pyrrhotite at bottom part of the picritic horizon (1665.4 m). The concentration of copper in sugakiite varies 0.48-0.90 wt.% (Table. 1. Nos. 25-28, Fig 7 a); this composition is similar to the first discovery described in Hokkaido (Kitakaze, 2008).

Disseminated ore in the taxitic gabbro-dolerite (RT-107_1698) is represented by monoclinic pyrrhotite, chalcopyrite, cubanite, and pentlandite. Ag-rich pentlandite (0.40-0.56 apfu Ag) and argentopentlandite (0.98-1.02 apfu Ag). The Ag concentration in the latter reaches 13.16 wt. %. (Table. 1, 56-61), and Fe significantly prevails over Ni (Table. 1, Fig. 7 c). Argentopentlandite grains (about 100 mμ) are included in the chalcopyrite matrix in association with fine Ag-free pentlandite grains framing this chalcopyrite (Table 1, fig. 8 a,b,f).

Massive ore of the southern orebody (RT-30_1566) are characterized by the predominance of pyrrhotite over other sulfides. Pentlandite occurs in two generations: Pn_1 as rims around chalcopyrite segregations, and Pn_2 as thin lamellae - exsolution inclusions in a pyrrhotite matrix. Pentlandite contains a ubiquitous of Ni up to 1 wt.%, and Co from 1.42 to 1.80 wt. %. Compositions of pentlandite vary within the small limits and belong to both Fe-rich and Ni-rich varieties (Fig. 7 c). Compositions intermediate between cubanite and chalcopyrite are, possibly the finely exsolution texture between these minerals (Fig. 7 d).

3.3. Association of Minerals of Platinum Group Elements (PGM)

Disseminated ore in the picritic gabbro-dolerite of the southern orebody (RT-30_1527) contains the following PGMs: sperrylite $PtAs_2$ grains (30-50 μm) intergrown with chalcopyrite and pentlandite (Fig. 9 a, c, i), Te- and Sb-bearing sobolevskite Pd(Bi, Te, Sb) (Fig. 9 b,f,g), sopcheite $Ag_4Pd_3Te_4$ as a small (2 μm) inclusion in pentlandite (Fig. 9 e), stibiopalladinite Pd_5Sb_2 intergrown with sobolevskite, and stannopalladinite Pd_5Sn_2Cu (Fig. 9 g,h) and single grains of Au-Ag alloys (Fig. 9 d). Stannopalladinite from the southern orebody contains Pt up to 7.52 wt. %, sometimes Sb about 2 wt.%, and corresponds to the formula $(Pd,Pt)_5(Sn,Sb)_2Cu$ (Fig. 10 a). Sperrylite and stibiopalladinite correspond to their stoichiometric $PtAs_2$ and Pd_5Sb_2 formulas, while sobolevskite Pd(Bi, Te, Sb) forms solid solutions with kotulskite up to 0.38 apfu Te and sudburyite up to 0.09 apfu Sb (Table 2).

https://doi.org/10.1180/mgm.2024.20 Published online by Cambridge University Press

The PGM association in disseminated ore in the picritic gabbro-dolerite of the northern orebody (PT-107) differs from those described above and includes niggliite PtSn with gold dissemination (Fig. 11 a) in the upper part of the horizon; atokite-rustenburgite solid solutions that dominate in the lower part of this horizon (Figs 11 f, i); paolovite Pd_2Sn, sometimes as a fine exsolution texture with sobolevskite (Fig. 11 h) and minerals intermediate in composition between taimyrite and cabriite (Fig. 10 a). Sperrylite is a common mineral of this association. Characteristic feature of PGM is an Au impurity (up to 5.77 wt. %) in atokite and rustenburgite (Table 2). Native silver, Ag-Au-Cu alloys, and auricupride Cu_3Au are common (Table 3, Fig. 12). In the taxitic gabbro-dolerite (in studied samples), only As-bearing paolovite was found up to 0.36 apfu As (Table 2).

Precious metal (PGE and Au) minerals from massive pyrrhotite ores are characterized by platinum specialization, i.e. all found PGMs are platinum minerals, even though Pd prevails over Pt in all ore samples. They form small (1-3 microns) inclusions in pyrrhotite, less often in chalcopyrite. These are represented by Pt-Fe alloys, platarsite PtAsS, sperrylite$PtAs_2$, and cooperite PtS (Fig. 13). Small size of these grains does not always allow to obtain the quantitative composition of the minerals, but they are qualitatively identified. Only the Au-Ag alloys and cooperite reach 15-25 μm (Fig. 13 a,g). The Au-Ag alloys of this association are high-grade gold compared to those from picritic rocks: $Au_{0.64}Ag_{0.36}$ (Table. 3, Fig. 12). The concentrations of both Pd and Ni do not exceed 1 wt.% in cooperite (Table 2). A rare associated mineral is bismuth oxychloride with the formula $BiOCl_2$, close to bismoclite (BiOCl) and acanthite Ag_2S, which occur as inclusions up to 10 μm in pyrrhotite of massive ores (Fig. 13 h, i).

4. DISCUSSION

4.1. Mineralogical feature and zoning in picritic gabbro-dolerite of C-3 and C-4 orebodies

The mineralogy of various types of ores of the Norilsk deposits has been studied and discussed for many years (for example, Genkin et al., 1969, 1981; Distler et al., 1975, 1999; Genkin and Evstigneeva, 1986; Begizov et al., 1974; Razin et al., 1976; Evstigneeva and Genkin, 1983; Barkov et al., 2000; Kozyrev et al., 2002; Komarova et al., 2002; Spiridonov et al., 2003, 2004, 2015; Likhachev, 2004; Sluzhenikin, 2010, 2011; Sluzhenikin and Mokhov, 2014; Tolstykh et al., 2020a,b, 2021) and many others). Our conclusions is based on mineralogical data that allow to evaluate the physicochemical conditions of ore crystallization, in particular, fugacity of sulfur in the ore-forming system during the formation of ores.

The southern and northern orebodies differ in mineralogical composition. The southern C-4 orebody is characterized by a high-sulfur association and zoning, expressed by pyrrhotite-chalcopyrite fractionation (Distler et al., 1975), and the northern C-3 orebody contains minerals

https://doi.org/10.1180/mgm.2024.20 Published online by Cambridge University Press

typical of a low-sulfur association (troilite, talnakhite, sugakiite) which is a characteristic of disseminated ores in the picritic gabbro-dolerite only (Distler et al., 1999; Tolstykh et al., 2017).

Moreover, these orebodies show multidirectional zoning in pentlandite compositions (Fig. 7), which regularly varies along the sections of the intrusive rocks. Fe/Ni ratio in pentlandite reflects the activity of sulfur ($lgfS_2$) during its formation, and the Ni content in pentlandite has direct proportional dependence of $lgfS_2$ (Kaneda et al., 1986; Kolonin et al., 2000; Kosyakov et al., 2003). This dependence is based on the experimental data and calculation of k = Ni/(Ni + Fe) in pentlandite (Fig. 14). The value «k» varies from 0.38 (in both boreholes, i.e., RT-30 and RT-107), which corresponds to the lowest values $logfS_2$ (-13) in the pentlandite stability field, to 0.52 ($logfS_2$ = -10.5) in RT-30 and up to 0.54 ($lgfS_2$ = - 10) in RT-107. These evolution vectors are multidirectional in sections of picritic rocks from different orebodies of the Oktyabr'sky deposit (Fig. 15). Our data evidence that the Ni/(Ni+Fe) ratio in pentlandite and S in pyrrhotite increase with depth in disseminated ore of the southern body (borehole RT-30 from 1501.2 m to 1527 m), consequently, the fugacity of sulfur increase and the evolution of the sulfide melt occurs in the same direction. Whereas the picritic gabro-dolerite from borehole RT-107 (northern C-4 orebody) shows opposite zoning: Fe-enriched pentlandite and troilite are characteristic of the deeper 1665.4 m horizon, and the Ni/(Ni+Fe) ratios in pentlandite increase up section (Fig. 7 a,b). Consequently, the evolution of the sulfide melt increases from bottom to top along the picritic rock of C-3 orebody (reverse zoning).

Mineralogical zoning in picritic gabbro-dolerite was also described earlier: from a low-sulfur association with troilite, talnakhite, cubanite, and Fe-rich pentlandite in the upper, most magnesian part, to a high-sulfur association at its base (Distler et al., 1999). The same direction of evolution of sulfide parageneses from top to bottom was observed in picritic gabbro-dolerite of the Norilsk 1 intrusion (Tolstykh et al., 2020b, 2021). Sluzhenikin (2010) showed that in picritic rocks zoning is directed in both directions from the central part towards the top and bottom, but also with a relative increase in the sulfur content of parageneses.

The zoning of disseminated ores in different boreholes that we identified coincides with the evolution vectors shown for the similar in composition massive sulfide lenses (Torgashin, 1994; fig. 3). These massive lenses also have opposite vertical mineralogical and geochemical zoning: the lenses of cubanite-chalcopyrite ore is characterized by an increase in incompatible elements from bottom to top along the section similar to the southern C-3 orebody). Whereas the ores in the pyrrhotite domain, on the contrary, evolve from top to bottom - along the vertical section as in northern C-4 orebody.

4.2. Minerals of platinum group elements from disseminated ore in the picritic gabbro-dolerite

https://doi.org/10.1180/mgm.2024.20 Published online by Cambridge University Press

The compositions of disseminated ores from different rocks and the paragenesis of sulfide minerals in the picritic and taxitic gabbro-dolerites have been established for the Norilsk 1, Oktyabr'sky and Talnakh deposits (Genkin et al., 1977; Naldrett, 2004; Distler et al., 1979, 1999; Spiridonov, 2010; Tolstykh et al., 2020b, etc.). Sometimes disseminated ores in picritic and taxitic gabbro-dolerites are combined during research and considered together as one «Main Ore Horizon» (Komarova et al., 2002).

Using the example of the Norilsk 1 intrusion, we showed (Tolstykh et al., 2021) that picritic and taxitic gabbro-dolerites differ in mineral associations, but at the same time they are characterized by the same type of zoning in relation to PGMs: from Pd-Sn-Cu minerals common in the upper parts of both layers to the minerals of Pd-Bi-Sb and Pd-Bi systems characteristic of the base of each layer, in accordance with the regressive temperature gradient and the direction of PGE fractionation in the sulfide melt. Such a distribution of PGMs characterizes the reverse zoning.

The studied PGM associations in the C-3 and C-4 orebodies are also unevenly distributed: at the base of the picritic gabbro-dolerite of C-4 orebody, the leading minerals are high-temperature PGMs of the Pd-Pt-Cu-Sn system: atokite-rustenburgite $(Pd,Pt)_3Sn$, cabriite Pd_2CuSn and paolovite Pd_2Sn, which corresponds to direct zoning. Whereas at the base of picritic gabbro-dolerite of C-3 orebody, low-temperature PGMs of the Pd-Bi-Te-Sb system sobolevskite Pd(Bi,Te) are widespread in accordance with the reverse zoning of the development of the ore-forming system (Fig. 15).

The modes of occurrences of Au and Ag also differ: only silver telluride (sopcheite) was found in the southern C-3 orebody, while native alloys (Ag, Au, Cu) are typical for the northern C-4 orebody which are enriched in Au at a higher level. Thus, the PGE-bearing ore-forming systems of picritic gabbro-dolerite differ in different orebodies of the Oktyabr'sky deposit, penetrated by RT-30 and RT-107 boreholes (Fig. 16 a,b).

4.3. Mineralogical similarities and differences between disseminated and massive ores in the southern orebodies.

Massive ore in the exocontact of the intrusion and disseminated ore in the picritic gabbro-dolerite of a section along the RT-30 borehole of the southern C-3 orebody have both differences and similarities. The main difference is in the features of PGM mineralization. While the Pd-Bi-Sb-Te minerals are common in the disseminated ores, massive ores contain only Pt minerals, among which cooperite PtS is more common (Fig. 16 c). This specificity of massive ores makes them comparable with other pyrrhotite ores of the Norilsk region (Kozyrev et al., 2002), but not with disseminated ores in the picritic rocks.

https://doi.org/10.1180/mgm.2024.20 Published online by Cambridge University Press

Nevertheless, the similarity lies in the unidirectional mineralogical and geochemical zoning from top to bottom along the cross-section, due to the evolution of sulfide melt (Fig. 15). It is assumed that zoning in the pyrrhotite ores of the C-3 body is analogous to zoning in the pyrrhotite lens of the Main Ore Body of the Oktyabr'sky deposit, where the concentration of Cu and incoherent elements increases down the section (Torgashin, 1994, Fig. 3).

This unidirectional evolution seems logical if one adheres to the idea that massive ores are the result of the deposition of sulfide droplets from disseminated horizons and their infiltration into the underlying rocks through the taxitic and contact gabbro-dolerite. Barren hornfelses at the contact of disseminated and massive ores, sharp changes in sulfide parageneses between picritic and taxitic gabbro-dolerites (Tolstykh et al., 2020b), as well as a significant difference in PGM associations between disseminated and underlying massive ores do not fit into this logic. If we consider disseminated and massive ores as different episodes of long-term magmatic activity (Zientek, Likhachev, 1992), then unidirectional trends (evolutionary zoning) of massive and disseminated ores can be caused by the action of similar mechanisms of intrusion of silicate magma (with droplets of sulfides) and sulfide melts.

4.4. Features of rare sulfides from various types of ores

Argentopentlandite $Ag(Ni,Fe)_8S_8$ occurs in taxitic gabbro-dolerite (RT-107_1695) of C-4 orebody. This mineral was found in various ores of the Norilsk deposits also, and it can be associated simultaneously with ordinary pentlandite and Ag-bearing pentlandite (Sluzhenikhin and Mokhov, 2014), as in our case. Ag can only occupy an octahedral position in argentopentlandite, so its amount should not exceed 1 apfu of Ag in structure of mineral (Hall and Stewart, 1973; Rudashevskii et al., 1977), which corresponds to the formula $Ag(Fe,Ni)_8S_8$ or, more precisely, $AgFe^{2+}{}_6Ni_2S_8$, in which Fe predominates three times over Ni, which is also characteristic of the studied argentopentlandite (Table 1). Argentopentlandite may be a product of exsolution from Ag-bearing Iss during the cooling of the ore-forming system according to one of the models described in (Melfos et al., 2001). Taking into account its morphological features, namely, segregations as relatively large grains (60-70 μm) in the chalcopyrite matrix, located in the halo of small Ag-free pentlandite grains (Fig. 8), it can be assumed that argentopentlandite is an early mineral and crystallizes under the less sulfuric conditions of the ore-forming system of the taxitic gabbro-dolerite. Then, with a decrease in temperature and an increase in sulfur fugacity, small grains of more nickel-rich pentlandite crystallized from residual melts in the intergranular space of surrounding chalcopyrite grains, the composition of which corresponds to the $\log fS_2 = -10 - -10.5$.

Sugakiite as large (around 80 μm) granular grains are common in the picritic gabbro-dolerite of C-4 orebody. It is assumed that sugakiite crystallized due to the peritectic reaction of Mss with

https://doi.org/10.1180/mgm.2024.20 Published online by Cambridge University Press

melt, similar to early pentlandite Pn_1 (Distler et al., 1996), but only under conditions of low sulfur activity, which is noted at the base of the picritic rocks in RT-107 borehole. Sugakiite is not the exsolution product, since this mineral contains copper up to 0.9 apfu Cu that is in excess in the residual melt, but does not fractionate in Mss. The ratio Ni/(Ni+Fe) in sugakiite is the lowest (0.26-0.27) compared to pentlandite of all horizons of the picritic rock in RT-107 borehole. Compositions of sugakiite are most shifted to the ferruginous area of the diagram (Fig. 7 a). This mineral intergrows with troilite, so, it can be assumed that it crystallized under the conditions of the lowest sulfur fugacity values that were achieved at the base of the picritic layer of the C-4 orebody. Sugakiite is a very rare mineral of low sulfur association discovered in sulfide aggregates in a peridotite of the Horoman massif, Hokkaido, Japan (Kitakaze, 2008). Sugakiite was also noted in picritic gabbro-dolerite of the C-6 orebody located in the northeastern part of the Oktyabr'sky deposit, whose massive ores are also essentially pyrrhotite (Ketrov et al., 2022).

4.5. Origin of different types of sulfide ores

There is an idea that the Kharaelakh intrusion is a single horizontal channel of magma supply to the surface (chonolith), in which, upon interaction with the host rocks, a sulfide melt was segregated, forming ore bodies (Rad'ko, 1991). Other researchers have been suggested a two-stage (Zolotukhin et al., 1975), three-stage (Turovtsev, 2002; Malitch et al. 2010) or multipulse (Zientek and Likhachev, 1992; Likhachev, 1996) formation of the Kharaelakh intrusion. An extended period of magmatic activity from Middle Paleozoic to Early Mesozoic consistent with multiple magmatic events during the evolution of the Kharaelakh intrusion was assumed. The interaction of juvenile and crustal magmatic sources with a dominant role of mantle origin based on Hf-Nd isotope data was established (Malich et al., 2010). The multipulse idea is consistent with our mineralogical studies of the central part of the Oktyabr'sky deposit, where the intrusion and crystallization of differently fractionated melts was going on in the southern and northern orebodies. Each magma pulse generated its own cooling front on a local scale, forming forward zoning in the northern C-4 orebody, and reverse zoning in the southern C-3 orebody. The high ore/silicate disbalance and complex mineralogical and geochemical zoning confirms a dynamic mode of origin of ore-bearing intrusions and a pulsed nature of magma intrusion with different evolution of sulfide melts in C-3 and C-4 orebodies.

It is assumed that disseminated ores were formed as a result of the intrusion of silicate magma containing sulfide liquid, the segregation of which occurred throughout the entire period of existence of the magmatic melt (Zientek and Likhachev, 1992; Likhachev, 1973, 2006). Volatiles in magma played a significant role in the carrying capacity of rising magma transporting sulfide droplets. To explain the formation of glabular disseminated ores in picritic gabbro-

https://doi.org/10.1180/mgm.2024.20 Published online by Cambridge University Press

dolerites, models of the so-called “Segregation vesicles” attached to sulphide liquid droplets, are used. The segregation vesicles disruption occured in situ at low pressures, resulting in the release of sulfide liquids that could accumulate in traps. However, the "bubble-rafting" according to (Yao et al., 2019; Barnes et al., 2019) was not the predominant mechanism of ore formation. The mechanisms of evaporite assimilation in situ and high R-factor there is no need to involve for the formation of disseminated ores (Yao et al., 2019).

The formation of massive ores, according to A.P. Likhachev (2006) is the result of sulfide liquate settling in widened sections of magma channels, where magma flow slowed down. In our case, it is also unlikely that massive ores, in this case, could be a result of permanent settling of sulfide droplets to the bottom of the formation chamber and the penetration of the accumulated sulfide melt through the layers of taxitic and contact gabrodolerites into the underlying rocks. The arguments are: i) disseminated ores in picritic gabbro-dolerites and massive ores have completely different sulfide phase and PGM compositions; ii) there is a distinct geochemical and mineralogical contrast between picritic and underlying taxitic ores (Tolstykh et al., 2017, 2020b, 2021), rather than gradual changes in composition, as would occur with sequential droplet deposition; iii) there is a gap between disseminated and massive ores - the presence of a layer of barren rocks. There is also a hypothesis that disseminated ore in the gabbro-dolerites are enriched in "fractional sulfide fluid coming from underlying massive sulfide ores" (Naldrett, 2004). This seems unlikely since there is a layer of barren hornfelses between the massive ore and taxitic gabbro-dolerite (Fig. 5).

It is obvious that the formation of disseminated and massive ores are fragments of two different intrusion processes from one intermediate chamber since the geochemical features, namely the PGE distribution patterns, are the same for all types of ores, but with different degrees of element fractionation (Tolstykh et al., 2020b). It can be assumed that the magmatic system first functioned as an open, fills the pools in a single act in the case of direct zoning in C-4 orebody or multi-act in the case of reverse zoning in C-3 orebody. After that the magmatic system could close, giving preference to crystallization fractionation at the final stage.

The formation of reverse zoning in the marginal parts of layered intrusions is a controversial issue (Latypov et al., 2007, 2011; Latypov and Egorova, 2012; Egorova and Latypov, 2013; Egorova and Shelepayev, 2020 and references therein). The authors summarized numerous reasons leading to the reverse zoning were analyzed, suggesting top-down crystallization of ore matter: 1) the floating of early Mss crystals towards the roof; 2) a progressive decrease in the amount of trapped residual liquid; 3) top-down solidification from a cold roof rocks and other. However, these factors are debatable and and each of them in each specific case may be decisive.

https://doi.org/10.1180/mgm.2024.20 Published online by Cambridge University Press

In our opinion, the most appropriate petrological mechanisms of the reverse zoning formation is the filling of the magma chamber with the continuously arriving of increasingly primitive melt, which was fractionated in the supply channel or in the intermediate chamber (Egorova, Latypov, 2013). This mechanism is most consistent with the zoning in the C-3 orebody, and also that we observe in the rocks in the Norilsk 1 intrusion (Tolstykh et al., 2020b).

The process of fractional crystallization was most likely the leading one, since both types of zoning (direct and reverse) correspond to the evolution of the sulfide melt - in the first case in situ (in chamber of formation), in the second - in intermediate chamber or supply channel, if we accept the hypothesis of a continuous flow of increasingly primitive melts (Latypov et al., 2007, 2011).

CONCLUSION

1. The southern C-3 orebody of massive ores penetrated by RT-30 borehole, composed mainly of pyrrhotite composition, is comparable to the pyrrhotyte lenses while the northern C-4 orebody, composed of talnakhite-chalcopyrite ores penetrated by the RT-107 borehole, can compare with the Cu-rich lenses of Main Orebody (MOB) of Oktyabr'sky deposit.

2. The southern and northern orebodies differ in them of their mineral compositions.

The first one is characterized by a high-sulfur association, and the second one contains minerals with a deficit of sulfur. Multidirectional evolutions of ore-forming systems are observed in the disseminated ores of these deposits: in the northern C-4 orebody direct crystallization zoning is observed, where the fugacity of sulfur increases from bottom to top; whereas in the southern C-3 orebody fS_2 decreases in this direction. The identified zoning coincides with the evolution vectors of various «blocks» of massive MOB ores of the Oktyabr'sky deposit. The presence of the rare mineral sugakiite in the lower part of the picritic gabbro-dolerite of the northern orebody is confirmed by the extremely low values of sulfur fugacity, which increases up the section.

3. PGM associations and modes of occurrence of Au and Ag in the northern and southern orebodies also differ and correspond to sulfide zoning: in the lower horizon of picritic gabbro-dolerite of the northern orebody, the leading compounds are high-temperature PGM of Pd-Pt-Cu-Sn systems in accordance with direct zoning, while in the lower horizon of the southern orebody the low-temperature PGMs of the Pd-Bi-Te-Sb system are widespread in accordance with the reverse zoning of the evolution of ore-forming systems.

4. Disseminated and massive ores within a single cross-section of RT-30 borehole of the southern orebody are different in mineral associations: the former is characterized by minerals of

https://doi.org/10.1180/mgm.2024.20 Published online by Cambridge University Press

the Pd-Bi-Sb-Te system, while the latter is characterized only by Pt-minerals. The similarity of these ores lies in the unidirectional reverse mineralogical and geochemical zoningalong the cross-sections in both: in disseminated and massive ores, which are the result of different magmatic events. However, unidirectional zoning of both types of ores may be due to the action of the same type of mechanism.

5. All the above results indicate that the formation of the southern C-3 and northern C-4 orebody was in different physicochemical conditions as the result of intrusion of various portions of both ore-silicate magma, from which disseminated ores were formed, and sulfide melt, previously separated into copper-rich and iron-rich fractions in the intermediate chamber. And each of the portions entered the formation chambers through different magma channels.

Acknowledgments: Acknowledgments: We thank analysts M. Khlestov for carrying out analytical procedures and providing quantitative analyses, and N. Belkina and M. Podlipsky for technical assistance in the manuscript preparing.

Funding: This research was carried out within the framework of the state assignment of the IGM SB RAS financed by the Ministry of Science and Higher Education of the Russian Federation, and project of the Ministry of Science and Higher Education of the Russian Federation No. 13.1902.21.0018.

References

Barkov A., Martin R., Poirier G., Tarkian M., Pakhomovskii Y. and Men'shikov Y. (2000) Tatyanaite, a New Platinum-Group Mineral, the Pt Analogue of Taimyrite, from the Noril'sk Complex (Northern Siberia, Russia). *European Journal of Mineralogy*, **12**, 391–396.

Barnes S.J., Vaillant M.L., Godel B. and Lesher C.M. (2019) Droplets and Bubbles: Solidification of Sulphide-rich Vapour-saturated Orthocumulates in the Norilsk-Talnakh Ni–Cu–PGE Ore-bearing Intrusions. *Journal of Petrology*, **60(2)**, 269–300.

Barnes S.J., Zientek M.L. and Severson M.J. (2011) Ni, Cu, Au and platinum-group element contents of sulphides associated with intraplate magmatism: a synthesis. *Canadian Journal of Earth Sciences*, **34**, 337–351.

Begizov V.D., Meschankina V.I. and Dubakina L.S. (1974) Palladoarsenide Pd_2As – the new native palladium arsenide from the copper-Nickel Ores of Oktyabr'sky Deposit. *Zapiski Vsesoyuznogo Mineralogicheskogo Obshchestva*, **16**, 1294–1297 (in Russian).

Distler V.V. (1975) Zonality of copper-nickel ores of the Talnakh and Oktyabr'skoye deposits. *Geology of ore Deposits*, **2**, 16-26.

Distler V.V., Genkin A.D., Filimonova A.A., Hitrov V.G. and Laputina I.P. (1975) The zoning of copper-nickel ores of Talnakh and Oktyabr'sky deposits. *Geology of Ore Deposit*, **2**, 6–27 (in Russian).

Distler V.V., Grokhovskaya T.L., Evstigneeva T.L., Sluzhenikin S.F., Filimonova A.A. and Dyuzhikov O.A. (1988) *Petrology of Magmatic Sulphide Ore Formation*. Nauka, Moscow, Russia (in Russian).

https://doi.org/10.1180/mgm.2024.20 Published online by Cambridge University Press

Distler V.V., Kulakov A.A., Sluzhenikin S.F. and Laputina I.P. (1996) Quenched sulphide solid solutions in Noril'sk ores. *Geologe of Ore Deposit*, **38(1)**, 41–53 (in Russian).

Distler V.V., Sluzhenikin S.F., Cabri L.J., Krivolutskaya N.A., Turovtsev D.M., Golovanova T.I., Mokhov A.V., Knauf V.V. and Oleshkevich O.I. (1999) The platinum ore of the Norilsk layered intrusions: The ratio of magmatic and fluid concentration of noble metals. *Geology of Ore Deposits*, **41(3)**, 241–265 (in Russian).

Distler V.V., Smirnov A.V. and Grokhovskaya T.L. (1979) Stratification, latent layering of differentiated trap intrusions and conditions for the formation of sulfide mineralization. Pp. 211–292 in: *Conditions for the Formation of Magmatic Ore Deposits*. Nauka, Moscow, Russia (in Russian).

Dodin D.A. and Batuev B.N. (1971) Geology and Petrology of the Talnakh Differentiated Intrusions and their Metamorphic Aureole. Pp. 31-100 in: Urvantsev NN (ed.) Petrology and Resource Potencial of the Talnakh and Norilsk Differentiated Intrusions. Nedra, Leningrad, Russia (in Russian).

Dodin D.A., Sluzhenikin S.F. and Bogomolov M.A. (2009) *Ores and minerals of the Norilsk region.* Studio "Polyarnaya Zvezda", Moscow, Russia (in Russian).

Dyuzhikov O.A., Distler V.V., Strunin B.M., Mkrtychyan A.K., Sherman M.L. and Sluzhenikin S.F. (1992) Geology and metallogeny of sulfide deposits of Noril'sk region USSR. Society of Economic Geologists. Special Publication. 242 p.

Egorova V.V. and Latypov R.M. (2013) Mafic-Ultramafic Sills: New Insights from M- and S-shaped Mineral and Whole-rock Compositional Profiles. *Journal of Petrology*, **54(10)**, 2155–2190.

Egorova V.V. and Shelepaev R.A. (2020) Reverse zoning in the marginal zones of layered ultramafic-mafic intrusions using the example of the Mazhalyk peridotite-gabbro massif (southeastern Tuva). *Geosphere Research*, **3**, 17–33 (in Russian).

Evstigneeva T.L. and Genkin A.D. (1983) Cabriite Pd_2SnCu, a New Species in the Mineral Group of Palladium, Tin and Copper Compounds. *Canadian Mineralogist*, **21**, 481–487.

Genkin A.D. (1968) *PGM and their associations in Cu-Ni ores of Noril'sk deposits.* Nauka, Moscow, Russia (in Russian).

Genkin A.D. and Evstigneeva T.L. (1986) Associations of Platinum-Group Minerals of the Noril'sk Copper-Nickel Sulphide Ores. *Economic Geology*, **81**, 1203–1212.

Genkin A.D., Distler V.V., Gladyshev G.D., Filimonova A.A., Evstigneeva T.L., Kovalenker V.A., Laputina I.P., Smirnov A.V. and Grokhovskaya T.L. (1981) Sulphide Copper-Nickel Ores of the Noril'sk Deposits. Nauka, Moscow, Russia (in Russian).

Genkin A.D., Evstigneeva T.L., Troneva N.V. and Vyalsov N.L. (1969) Polarite Pd(Pb,B) - new mineral from copper-nickel sulfide ores. *Zapiski Vsesoyuznogo Mineralogicheskogo Obshchestva*, **6**, 708–715 (in Russian).

Genkin A.D., Kovalenker V.A., Smirnov A.V. and Muravitskaya G.N. (1977) Peculiarities of the mineral composition of Norilsk sulfide disseminated ores and their genetic characteristics. *Geology of Ore Deposits,* **1**, 24–35 (in Russian).

Geological Map of the Noril'sk region (1994) In: Strunin B.M. (ed.) *Explanatory notes to 1: 200000 geological map of the Noril'sk mining district*. St. Petersburg, VSEGEI (in Russian).

Godlevsky M.N. (1968) *Magmatic deposits*. Pp. 7-83 in Genesis of endogenous ore deposits. Nedra, Moscow, Russia (in Russia).

Gorbachev N. and Nekrasov A.N. (2004). Layering of Fe-Ni-Cu sulfide melts: Experimental study and geological implications. *Doklady Earth Sciences,* **399**, 1256–1259.

Gorbachev N.S. (2006) Mineralogical and geochemical zoning and genesis of massive sulfide ores at the Oktyabr'sky deposit. *Geology of Ore Deposits,* **48**, 473–488.

Hall S.R. and Stewart J.M. (1973) The crystal structure of argentian pentlandite $(Fe,Ni)_8AgS_8$, compared with the refined structure of pentlandite $(Fe,Ni)_9S_8$. *Canadian Mineralogist,* **12**, 169–177.

https://doi.org/10.1180/mgm.2024.20 Published online by Cambridge University Press

Kalugin V. and Latypov R. (2010) Two-Stage Formation of the Oktyabr'sky Sulfide Orebody, Noril'sk: Evidence From Vertical Chemical Zonation. In *11th International Platinum Symposium*. Ontario Geological Survey, Miscellaneous Release–Data 269.

Kalugin V. and Latypov. R (2012) Top-down fractional crystallization of a sulfide liquid during formation of largest ore-body from the Noril'sk-Talnakh PGE–Cu–Ni deposits, Russia. Geophysical Research Abstracts Vol. **14**, EGU2012-4135, 2012, EGU General Assembly.

Kalugin V.M. and Latypov R.M. (2009) Theoretical modelling of zoning of massive sulfide ores in the ternary system Cu-Fe-S. Pp. 213-216 in: *The third international conference «Mafic-ultramafic complexes of folded regions and related deposits»*. Ekaterinburg, Russia (in Russian).

Kaneda H., Takenouchi S. and Shoji T. (1986) Stability of Pentlandite in the Fe–Ni–Co–S System. *Mineralium Deposita*, **21**, 169–180. https://doi.org/10.1007/BF00199797

Ketrov A., Yudovskaya M.A., Shelukhina Yu.S., Velivetskaya T.A. and Palamarchuk R.S. (2022) Sources and evolution of the sulfur isotope composition of sulfides of the Kharaelakh and Pyasino-Vologochansky intrusions (Norilsk ore district). *Geology of Ore Deposits,* **64(6)**, 657–686 (in Russian).

Kitakaze A. (2008) Sugakiite, $Cu(Fe,Ni)_8S_8$, a new mineral from Hokkaido, Japan. *Canadian Mineralogist,* **46**, 263–267.

Kolonin G.R., Orsoev D.A., Sinyakova E.F. and Kislov E.V. (2000) The use of Ni: Fe ratio in pentlandite for estimation of sulfur fugacity during the formation of PGE-bearing sulfide mineralization of Yoko-Dovyren. *Doklady Earth Sciences*, **370**, 87–91 (in Russian).

Komarova M.Z., Kozyrev S.M., Simonov O.N. and Lyul'ko V.A. (2002) The PGE mineralization of disseminated sulphide ores of the Noril'sk-Taimyr Region. Pp. 547–567 in: Cabri L.J. (ed.) *The Geology, Geochemistry, Mineralogy and Mineral Beneficiation of Platinum-Group Elements*. Canadian Institute of Mining, Metallutry and Petroleum. Montreal, QC, Canada **54**.

Korolyuk V.N., Usova L.V. and Nigmatulina E.N. (2009) On the Accuracy of Determining Composition of Principal Rock-Forming Silicates and Oxides with a Jeol JXA-8100 Electron Microprobe. *Journal of Analytical Chemistry*, **64**, 1070–1074.

Kosyakov V.I., Sinyakova E.F. and Shestakov V.A. (2003) The Dependence of Fugacity of Sulphur from the Composition of Phase Associations of Fe–FeS–NiS–Ni at 873 K. *Geochemistry International*, **7**, 730–740 (in Russian).

Kozyrev S.M., Komarova M.Z., Emelina L.N., Oleshkevich O.I., Yakovleva O.A., Lyalinov D.V. and Maximov V.I. (2002) The mineralogy and behaviour of PGM during processing of the Norilsk-Talnakh PGE-Cu-Ni ores. Pp. 757–791 in: Cabri L.J. (ed.) *The Geology, Geochemistry, Mineralogy and Mineral Beneficiation of Platinum-Group Elements.* Canadian Institute of Mining, Metallurgy and Petroleum. Montreal, QC, Canada **54**.

Krivolutskaya N., Bychkova Y., Gongalsky B., Kubrakova I., Tyutyunnik O., Dekunova E. and Taskaev V. (2021) New Geochemical and Mineralogical Data on Rocks and Ores of the NE Flank of the Oktyabr'skoe Deposit (Norilsk Area) and a View on Their Origin. *Minerals*, **11(1)**, 44.

Krivolutskaya N., Gongalsky B., Kedrovskaya T., Kubrakova I., Tyutyunnik O., Chikatueva V., Bychkova Y., Magazina L., Kovalchuk E., Yakushev A. and Kononkova N. (2019) Geology of the western flanks of the Oktyabr'skoe deposit, Noril'sk district, Russia: evidence of a closed magmatic system. *Mineralium Deposita*, **54**, 611–630.

Krivolutskaya N., Nesterenko M.., Gongalsky B., Korshunov D., Bychkova Y. and Svirskaya N (2018) Unique PGE-Cu-Ni Oktyabr'skoe Deposit (Noril'sk Area, Siberia, Russia): New Data on Its Structure and Mineralization. Pp. 253–255 in: *Conference of the Arabian Journal of Geosciences CAJG*. Petrogenesis and Exploration of the Earth's Interior.

Krivolutskaya N.A. (2014) *Evolution of trap magmatism and processes producing Pt-Cu-Ni mineralization in the Noril'sk area*. KMK Scientific Press, Moscow, Russia (in Russian).

https://doi.org/10.1180/mgm.2024.20 Published online by Cambridge University Press

Kunilov V.Ye. (1994) Geology of the Nori lsk Region: The History of the Discovery, Prospecting, Exploration and Mining of the Noril'sk Deposits. *Sudbury-Noril'sk Symposium. Ontario Geological Survey Special Paper*, **5**, 203–216.

Latypov R.M. and Egorova V.V. (2012) Plagioclase compositions give evidence for in situ crystallization under horizontal flow conditions in mafic sills. *Geology*, **40**, 883–886.

Latypov R.M., Chistyakova S.Yu. and Alapieti T.T. (2007) Revisiting the problem of chilled margins associated with marginal reversals in mafic-ultramafic intrusive bodies. *Lithos*, **99**, 178–206.

Latypov R.M., Hanski E., Lavrenchuk A., Huhma H. and Havela T. (2011) A "three-increase model" for origin of marginal reversal in the Koitelainen layered intrusion, Finland. *Journal of Petrology*, **52**, 733–764.

Likhachev A.P. (1973) On the nature of magmatic deposits. *Soviet geology*, **5**, 33–47 (in Russian).

Likhachev A.P. (1994) Ore-bearing intrusions of the Noril'sk Region. Pp 185-201 in: Lightfoot P.C., Naldrett A.J. (eds.) *Proceedings of the Sudbury-Noril'sk Symposium*. Special Publication **5**. Geological Survey, Ontario.

Likhachev A.P. (1996) About dynamics of the formation of Talnakh ore-bearing intrusion and related Pt-Cu-Ni deposits. *Otechestvennaya Geologiya*, **8**, 20–26 (in Russian).

Likhachev A.P. (2004) On the possibility of platinum-copper-nickel ore formation in impact structures. *Domestic Geology*, 6, 3–12 (In Russian).

Likhachev A.P. (2006) *Platinum-copper-nickel deposits*. Elan, Moscow, Russia (in Russian).

Likhachev A.P. and Kukoev V.A. (1973) On melting and phase relations in sulfide, silicate and sulfide-silicate systems. *Geology of Ore Deposits*, **5**, 32–45 (in Russian).

Lul'ko V.A., Fedorenko V.A., Distler V.V. and Sluzhenikin S.F. (1994) Geology and ore deposits of the Norilsk region. P. 67 in: *Guidbook of VII International Platinum Symposium*. Moscovsky contact Press, Moscow, Russia.

Malich K.N., Belousova E., Griffin W., Badanina I., Pearson N., Presnyakov S., Tuganova E. (2010) Magmatic evolution of the ultramafic-mafic Kharaelakh intrusion (Siberian Craton, Russia): insights from trace-element, U-Pb and Hf-isotope data on zircon. *Contributions to Mineralogy and Petrology*, **159,** 753–768.

Melfos V., Vavelidis M. and Arikas K. (2001) A new occurrence of argentopentlandite and gold from the Au-Ag-rich copper mineralisation in the Paliomylos area, Serbomacedonian massif, Central Macedonia, Greece. *Bulletin of the Geological Society of Greece*, **34(3)**, 1065–1072.

Naldrett A.J. (2004) *Magmatic Sulphide Deposits: Geology, Geochemistry and Exploration*. Springer, Berlin, Heidelberg, 728 p.

Naldrett A.J., Asif M., Gorbachev N.S., Kunilov V.Ye., Stekhin A.I., Fedorenko V.A. and Lightfoot P.C. (1994) The Composition of the Ni-Cu Ores of the Oktyabr'sky Deposit, Noril'sk Region. Pp. 357-372 in Naldrett A.J., Lighfoot P.C., Sheahan P. (eds.) *The Sudbury-Norilsk Region Symposium Ontario Geological Survey*. Special Publication **5**. Geological Survey, Ontario.

Naldrett A.J., Fedorenko V., Shushen L., Asif M., Kunilov V.E., Stekhin A.I., Lightfoot P.C. and Gorbachev N.S. (1996) Controls on the composition of Ni-Cu sulsulfide deposits as illustrated by those at Noril'sk, Siberia. *Economic Geology*, **91**, 751–773.

Naldrett A.J., Fedorenko V.A., Lightfoot P.C., Kunilov V.E., Gorbachev N.S., Doherty W. and Johan Z. (1995) Ni-Cu-PGE deposits of the Noril'sk region, Siberia: their formation in conduits for flood basalt volcanism. *Institute if Mining and Metallurgy*, **104**, B18–B36.

Peregoedova A.V. (1999) *Physical and chemical behavior of Pt and Pd during crystallization of Fe, Ni, Cu-containing sulphide melts, and in subsequent subsolidus transformations*. Author. Dis. of kand. geol.-min. nauk, Novosibirsk (in Russian).

Rad'ko V.A. (1991) Model of dynamic differentiation of intrusive traps in the north-west of the Siberian Platform. *Geology and Geophysics*, **11**, 19–27 (in Russian).

https://doi.org/10.1180/mgm.2024.20 Published online by Cambridge University Press

Razin L.V., Dubakina L.S. and Dubinchuk V.T. (1976) Rhombic stannide of palladium, copper and platinum from copper-nickel sulfide ores of Norilsk-type deposits. *Zapiski Vsesoyuznogo Mineralogicheskogo Obshchestva*, **105(2)**, 206–213 (in Russian).

Rudashevskii N.S., Mintkenov G.A., Karpenkov A.M. and Shiskin N.N. (1977) Silver-containing pentlandite — the independent mineral species argentopentlandite. *Zapiski Vsesoyuznogo Mineralogicheskogo Obshchestva*, **106**, 688–691 (in Russian).

Sinyakova E.F., Borisenko A.S., Karmanov N.S. and Kosyakov V.I. (2019) Behavior of noble metals during fractional crystallization of Cu–Fe–Ni–(Pt, Pd, Rh, Ir, Ru, Ag, Au, Te) sulfide melts. *Russian Geology and Geophysics,* **60(6)**, 642– 661.

Sluzhenikin S.F. (2010) Platinum-copper-nickel and platinum ores of the Norilsk region and their ore mineralization. *Russian Chemical Journal*, **LIV2**, 38–49 (in Russian).

Sluzhenikin S.F. (2011) Platinum-copper-nickel and platinum ores of Noril'sk region and their ore mineralization. *Russian Journal of General Chemistry*, **81(6)**, 1288–1301.

Sluzhenikin S.F. and Mokhov A.V. (2014) Gold and silver in PGE-Cu-Ni and PGE ores of the Noril'sk deposits, Russia. *Mineralium Deposita*, **50(4)**. DOI 10.1007/s00126-014-0543-2

Spiridonov E.M. (2010) Ore-magmatic systems of the Noril'sk ore field. *Russian Geology and Geophysics*, **51(9)**, 1059–1077. DOI:10.1016/j.rgg.2010.08.011

Spiridonov E.M., Kulagov E.A. and Kulikova I.M. (2004) Palladium, platinum and gold mineral assemblages in ores of the Norilsk deposit. *Geologe of Ore Deposit*, **46(2)**, 150–166.

Spiridonov E.M., Kulagov E.A.., Serova AA., Kulikova I.M., Korotaeva N.N., Sereda E.V., Tushentsova I.N., Belyakov S.N. and Zhukov N.N. (2015) Genetic Pd, Pt, Au, Ag, and Rh mineralogy in Noril'sk sulfide ores. *Geology of Ore Deposits*, **57**, 402–432. https://doi.org/10.1134/S1075701515050062

Spiridonov E.M., Kulagov E.A.and Kulikova I.M. (2003) Pt-Pd tetraauricupride and associated minerals in ores of the Norilsk-I deposit. *Geology of Ore Deposits*, **45(3)**, 232–241.

Stekhin A.I. (1994) Mineralogical and chemical characteristics of the Cu-Ni ores of the Oktyabr'sky and Talnakh deposits. Pp. 217-230 in Lightfoot P.C., Naldrett A.J. (eds.) *Proceedings of the Sudbury-Noril'sk Symposium.* Ontario Geological Survey Special Volume 5.

Tolstykh N., Garcia J. and Shvedov G. (2021) Distribution of sulfides and PGE minerals in the picritic and taxitic gabbro-dolerites of the Norilsk 1 intrusion. *Canadian Mineralogist,* **59(6)**, 1437–1451. DOI:10.3749/canmin.2100037

Tolstykh N., Krivolutskaya N., Safonova I., Shapovalova M., Zhitova L. and Abersteinerd A. (2020a) Unique Cu-Rich Sulphide Ores of the Southern-2 Orebody in the Talnakh Intrusion, Noril'sk Area (Russia): Geochemistry, Mineralogy and Conditions of Crystallization. *Ore Geology Reviews*, **122**, 103525.

Tolstykh N., Shvedov G., Polonyankin A. and Korolyuk V. (2020b) Geochemical Features and Mineral Associations of Differentiated Rocks of the Norilsk 1 Intrusion. *Minerals*, **10(8)**, 688 https://doi.org/10.3390/min10080688

Tolstykh N.D., Shvedov G.I., Polonyankin A.A. and Zemlyanssky S.A. (2017) Mineralogical and geochemical feature of the disseminated ores of the southern part of the Noril'sk 1 deposit. *IOP Conf Series: Earth and Environmental Science*, **110**, 012021. DOI: 10.1088/1755-1315/110/1/012021

Torgashin A.S. (1994) Geology of the massive and copper ores of the western part of the Oktyabr'sky Deposit. *Sudbury–Noril'sk Symposium. Ontario Geological Survey Special Paper*, **5**, 231–241.

Turovtsev D.M. (2002) *Contact metamorphism of Norilsk intrusions*. Mir, Moscow, Russia. 318 p. (in Russian).

Valetov A.V., Badtiev B.P. and Ryabikin V.A. (2000) Present-Day State of Resource Base of the Noril'sk Mining Company. *Tsvetn Metally*, **6**, 10–14 (in Russian).

Vaughan D.J. and Craig J.R. (1981) *Mineral Chemistry of Metal Sulphides*. Nauchnyy Mir, Moscow, Russia (in Russian).

https://doi.org/10.1180/mgm.2024.20 Published online by Cambridge University Press

Yao Z., Mungall J.E. and Qin K.A. (2019) Preliminary Model for the Migration of Sulfide Droplets in a Magmatic Conduit and the Significance of Volatiles. *Journal of Petrology*, **60(12)**, 2281–2315.

Zientek M.L. and Likhachev A.P. (1992) Compositional constraints on the genesis of ore deposits of the Noril'sk-Talnakh distrtct' Siberia. P. 492 in *Abstracts of the Sudbury-Noril'sk symposium* (The Canadian Mineralogist).

Zientek M.L., Likhachev A.P., Kunilov V.E., Barnes S.-J., Meier A.L., Carlson R.R., Briggs P.H., Fries T.L. and Adrian B.M. (1994) Cumulus processes and the composition of magmatic ore deposits: examples from the Talnakh district, Russia. *Ontario Geological Survey Special Publication*, **5**, 373–392.

Zolotukhin V.V. (1964) Reaction aggregates in the Norilsk ores and the problem of disseminated sulfide mineralization in gabbro-dolerites. *Doklady Academy of Sciences USSR*, **154,** 600–603 (in Russian).

Zolotukhin V.V., Ryabov V.V., Vasil'ev Y.R. and Shatkov B.A. (1975) *Petrology of the Talnakh Differentiated Ore-Bearing Trap Intrusion*. Nauka, Novosibirsk, Russia (in Russian).

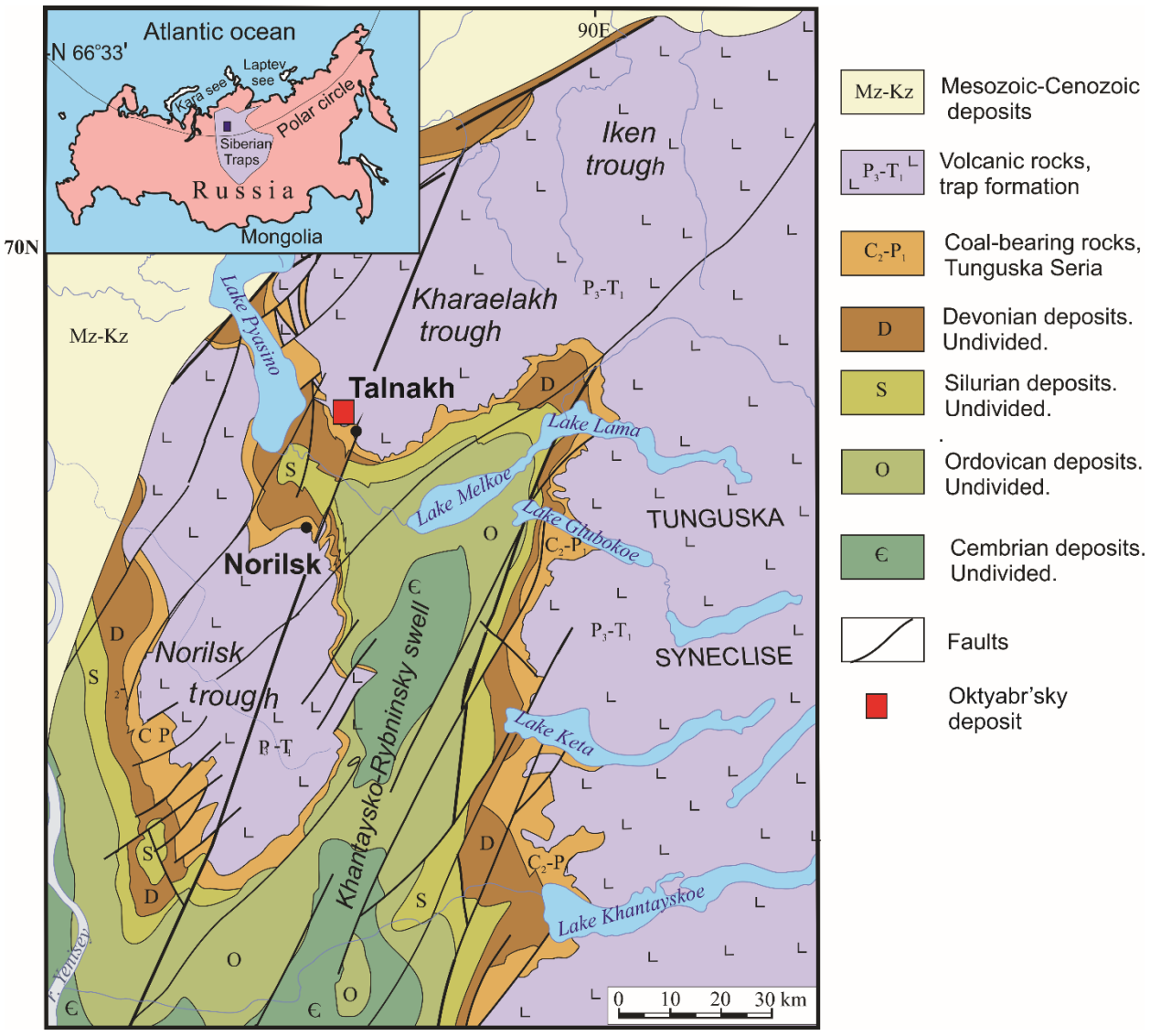

Figure 1.

https://doi.org/10.1180/mgm.2024.20 Published online by Cambridge University Press

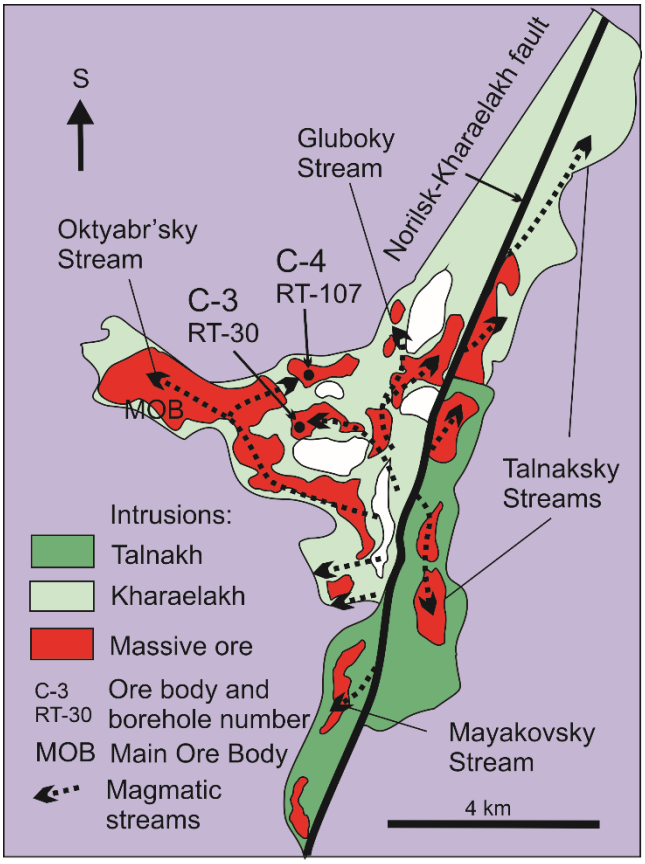

Figure 2.

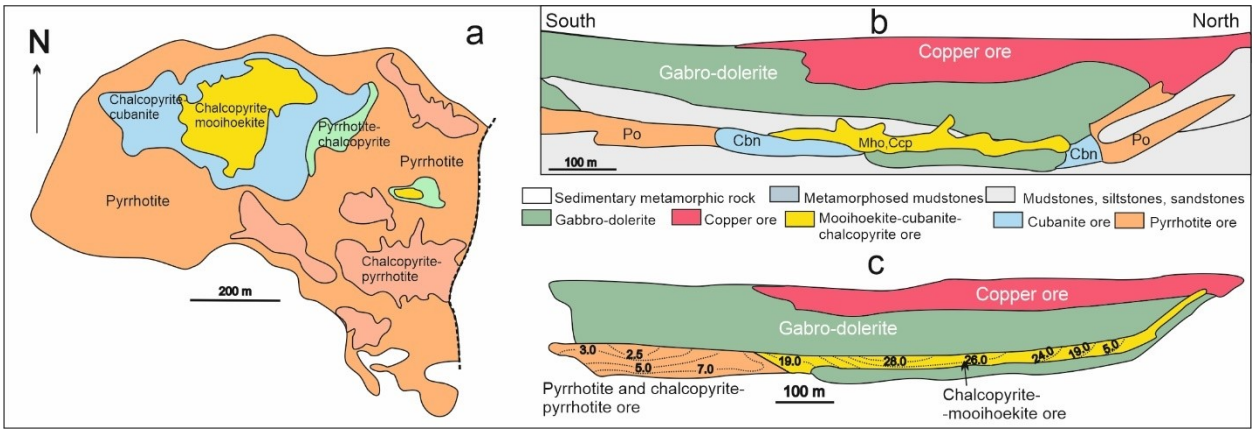

Figure 3.

https://doi.org/10.1180/mgm.2024.20 Published online by Cambridge University Press

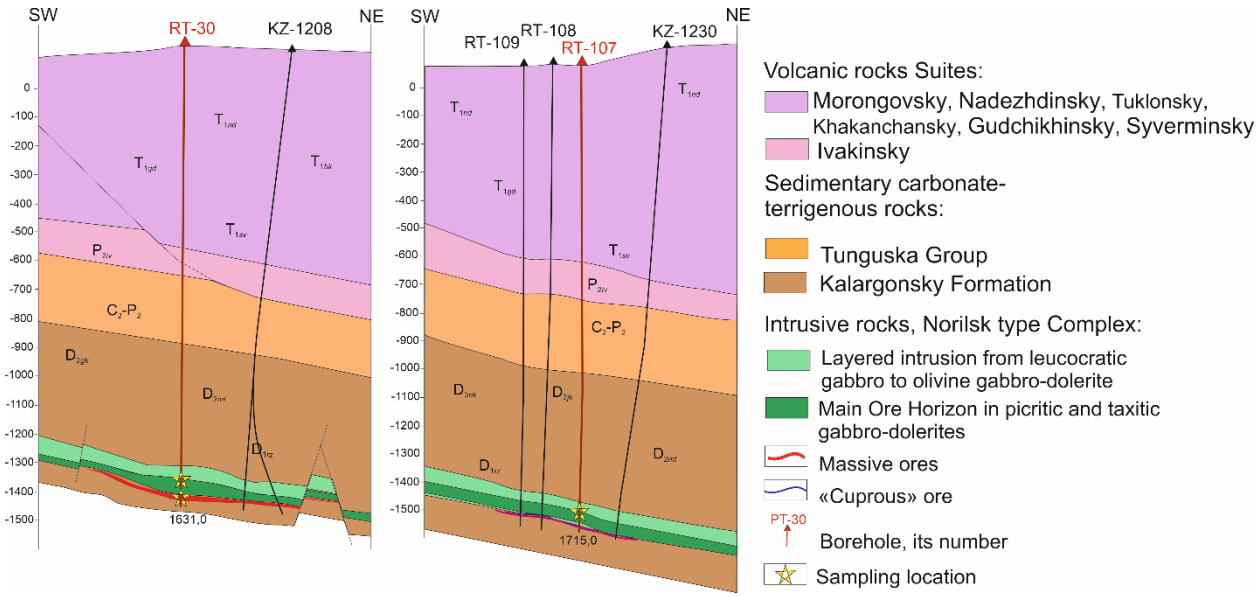

Figure 4.

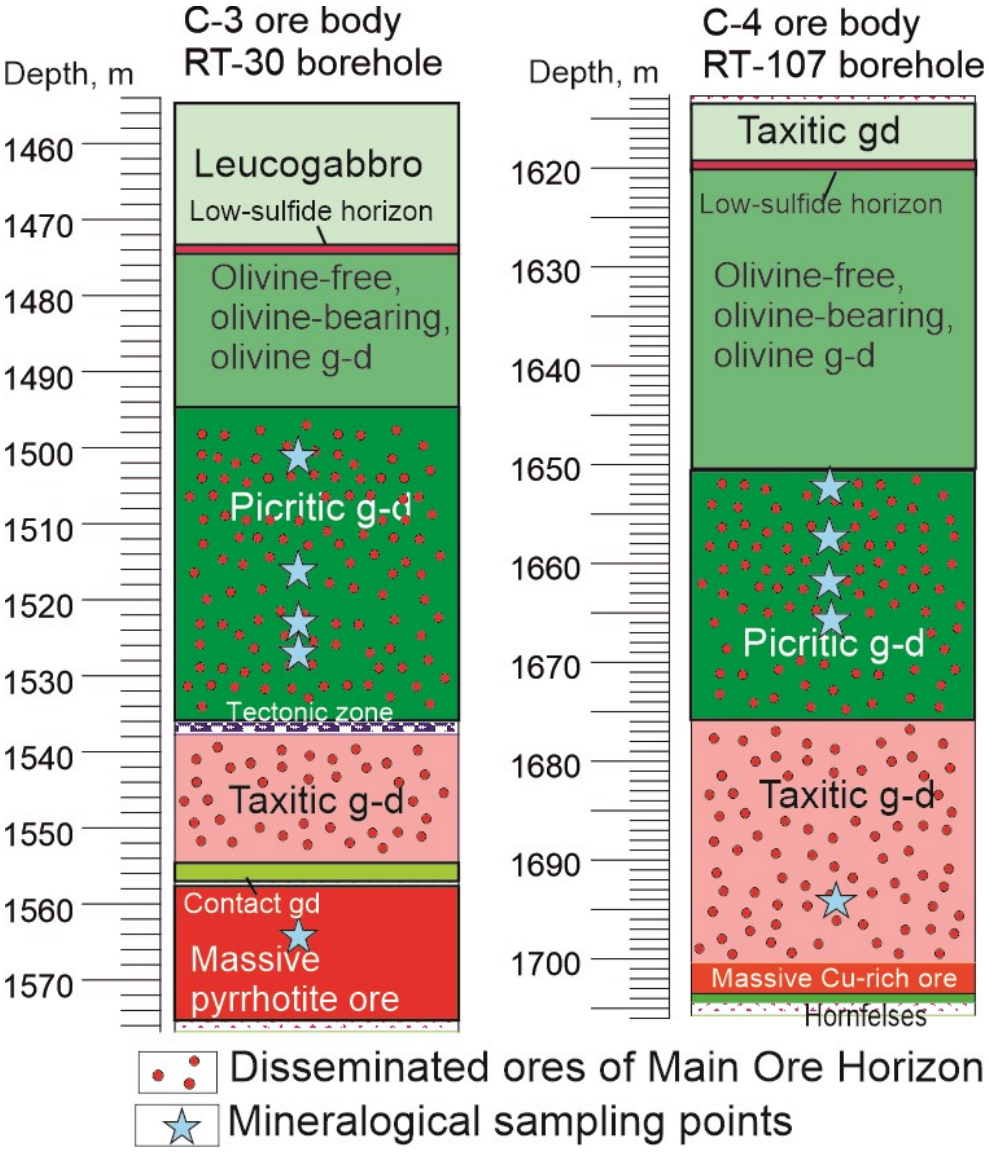

Figure 5.

https://doi.org/10.1180/mgm.2024.20 Published online by Cambridge University Press

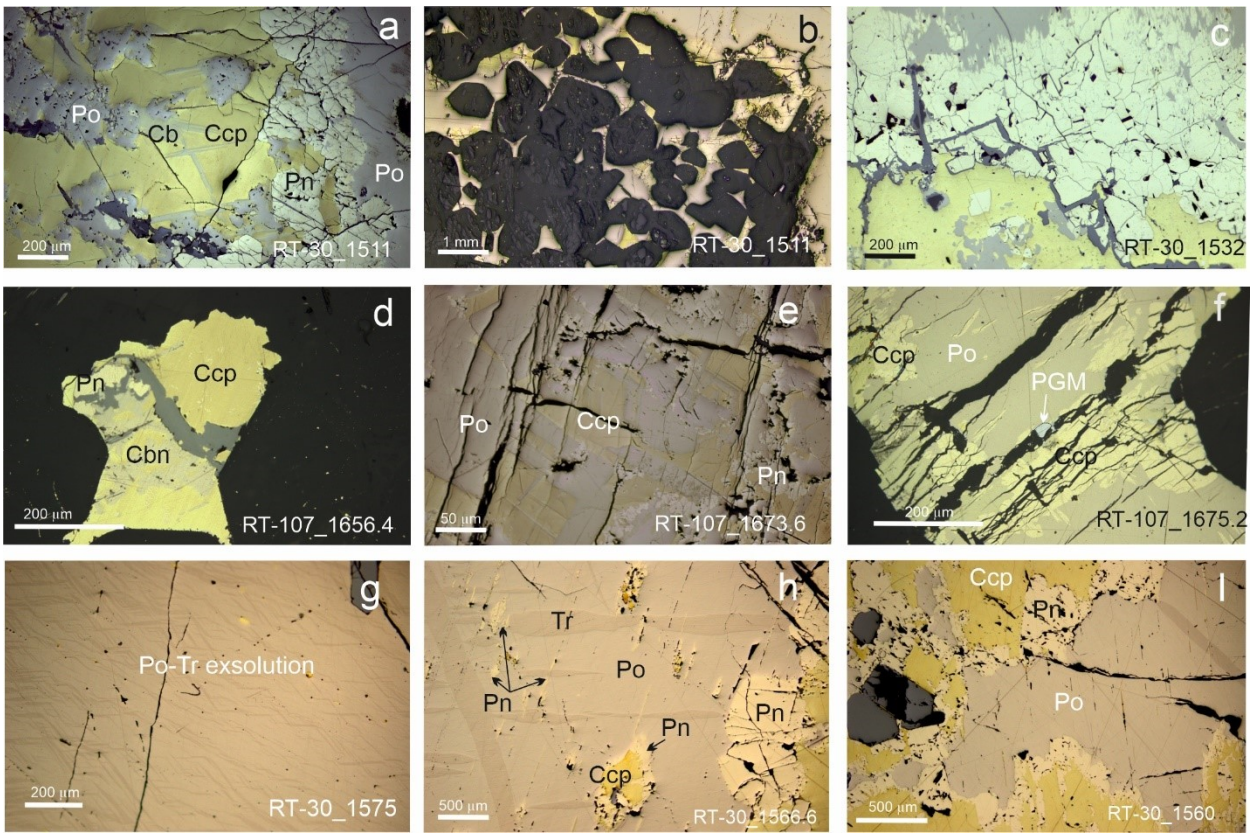

Figure 6.

https://doi.org/10.1180/mgm.2024.20 Published online by Cambridge University Press

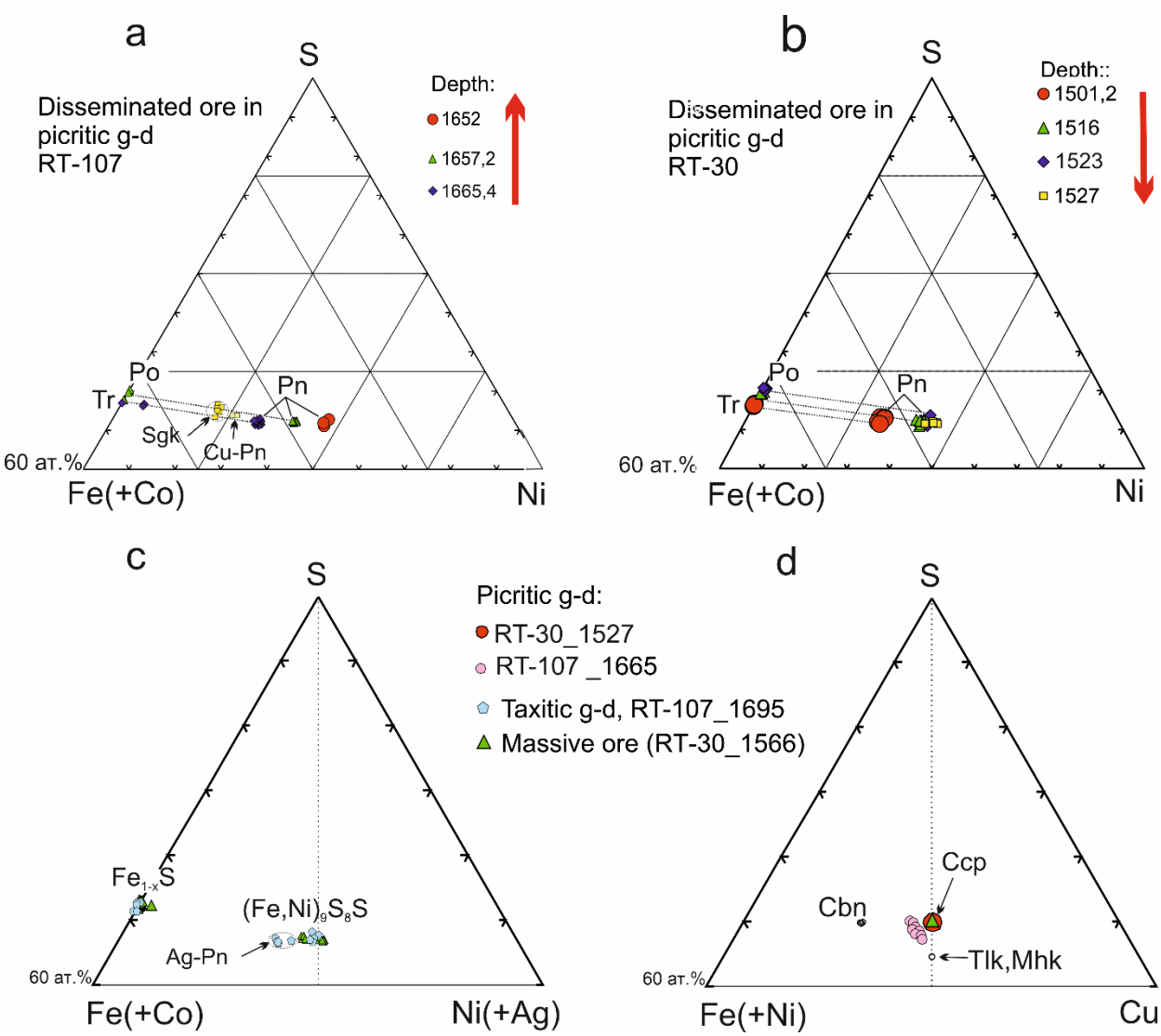

Figure 7.

https://doi.org/10.1180/mgm.2024.20 Published online by Cambridge University Press

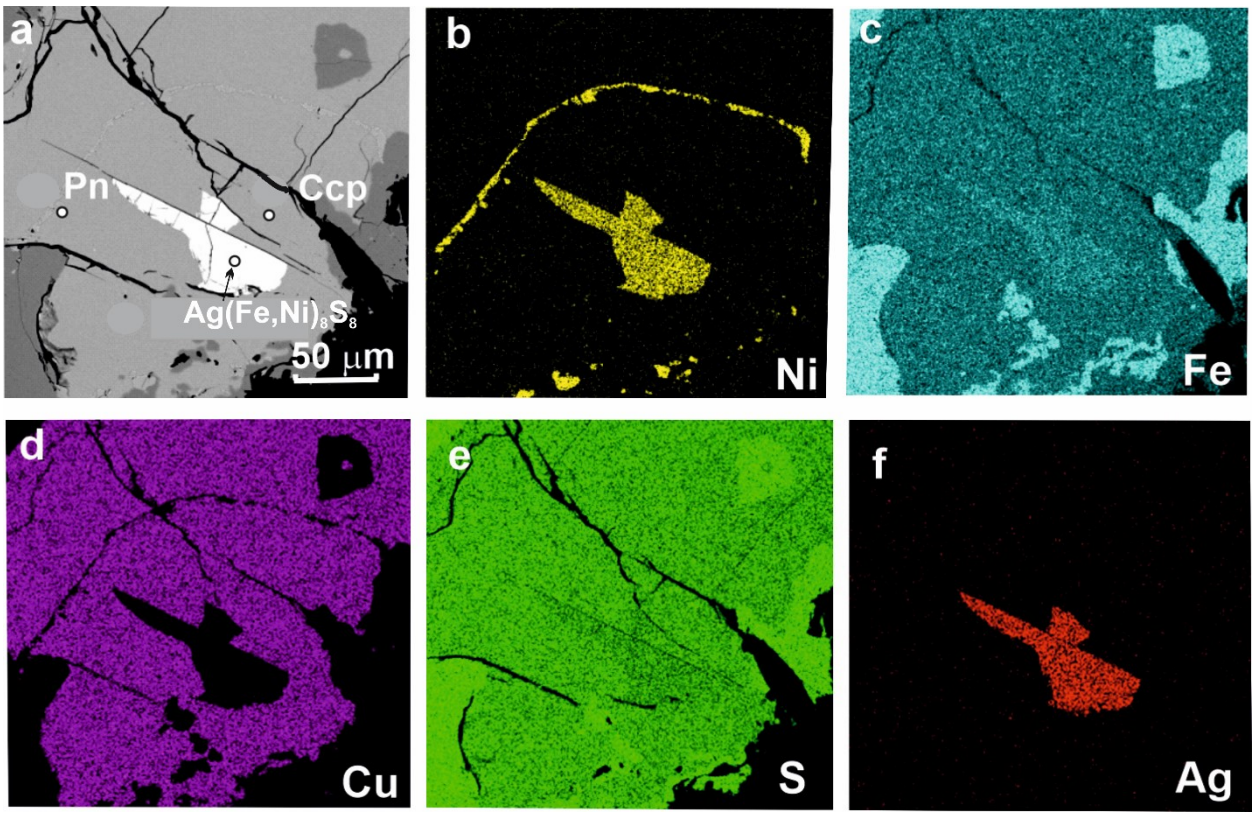

Figure 8.

https://doi.org/10.1180/mgm.2024.20 Published online by Cambridge University Press

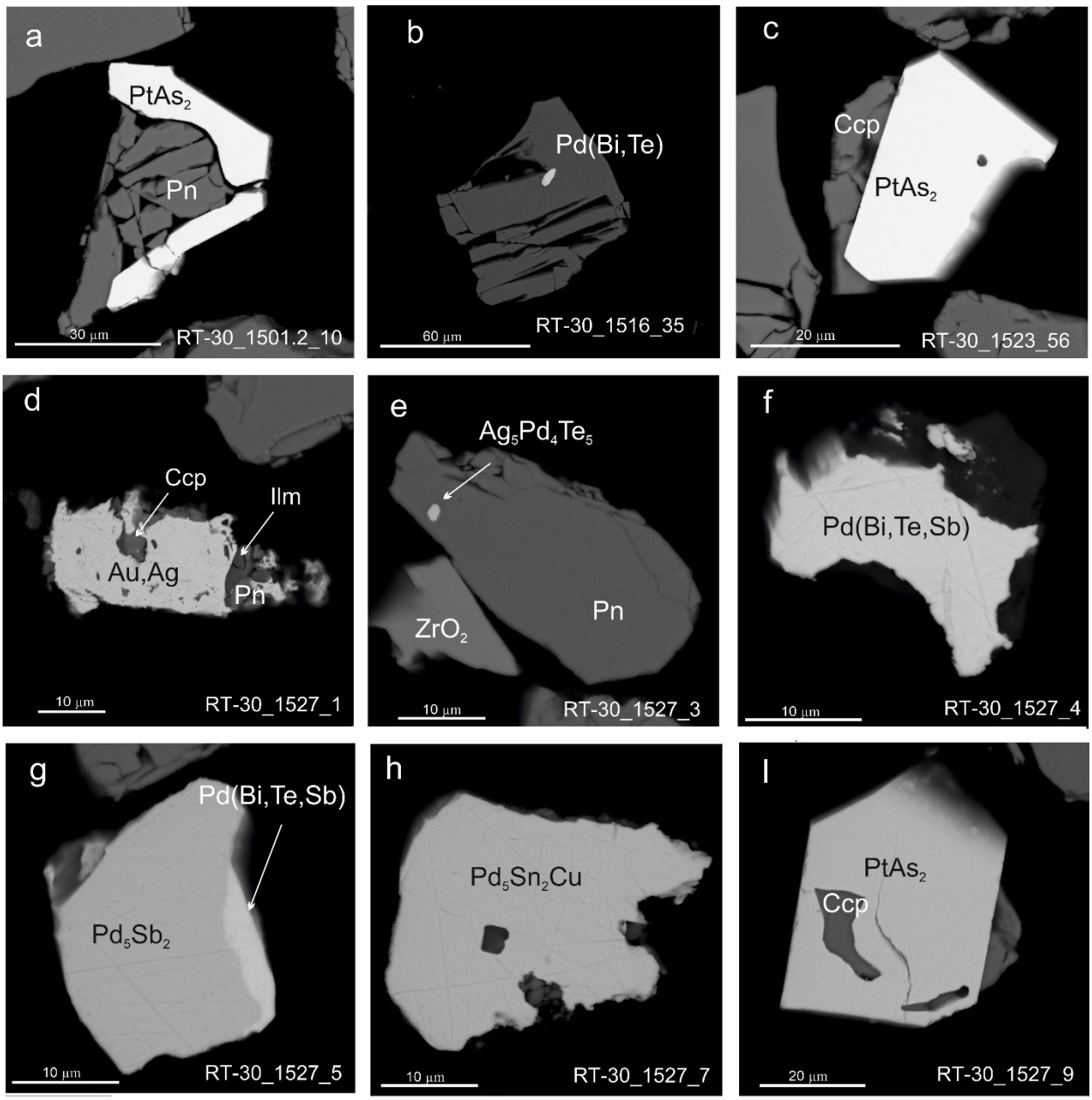

Figure 9.

https://doi.org/10.1180/mgm.2024.20 Published online by Cambridge University Press

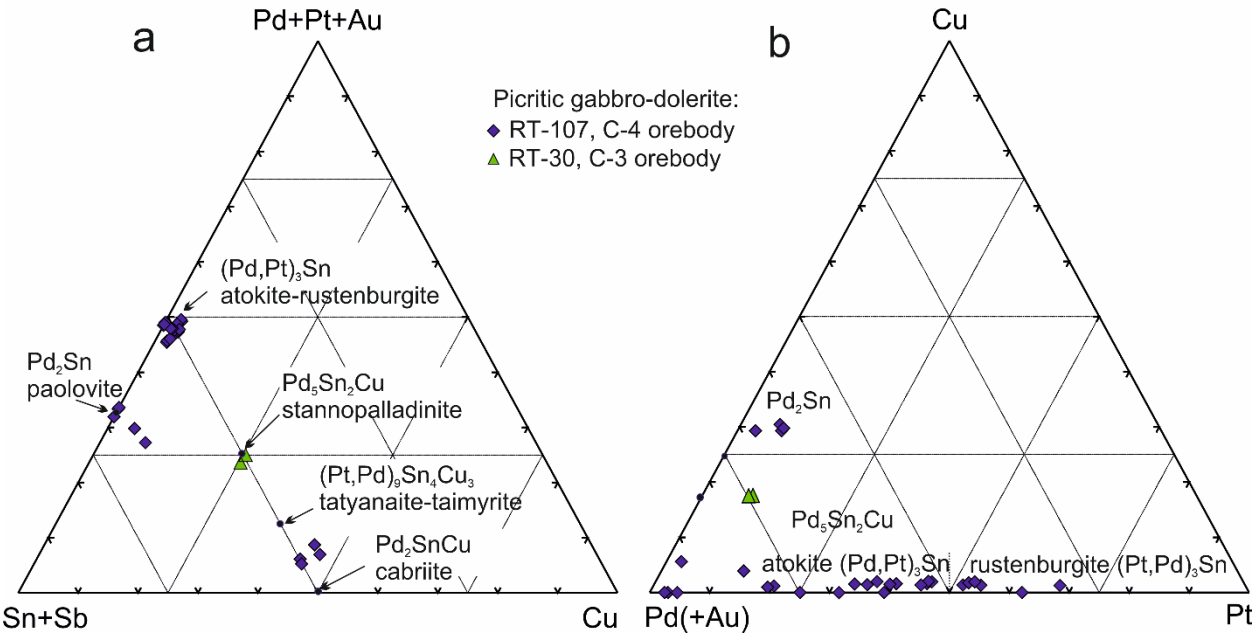

Figure 10.

https://doi.org/10.1180/mgm.2024.20 Published online by Cambridge University Press

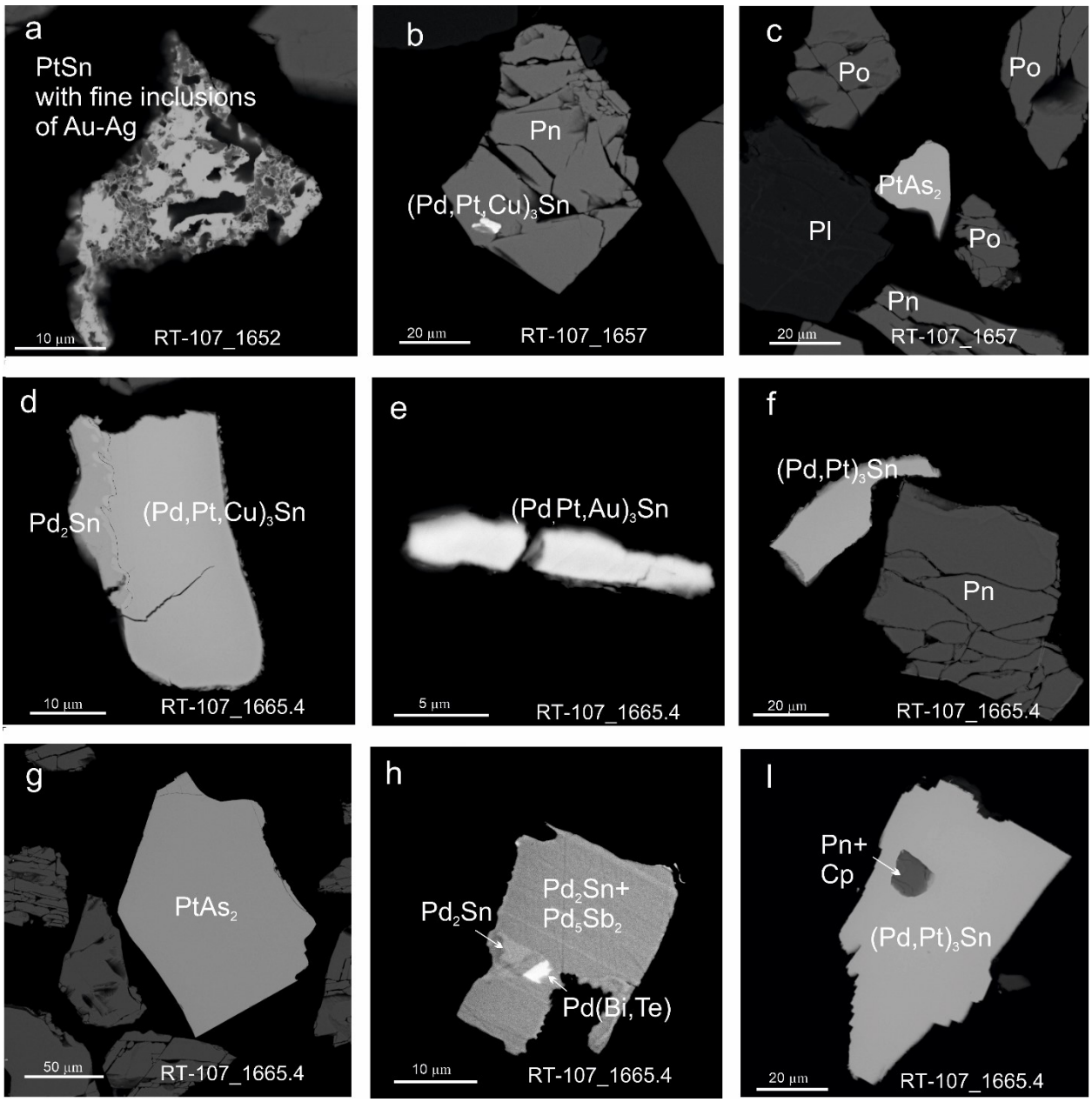

Figure 11.

https://doi.org/10.1180/mgm.2024.20 Published online by Cambridge University Press

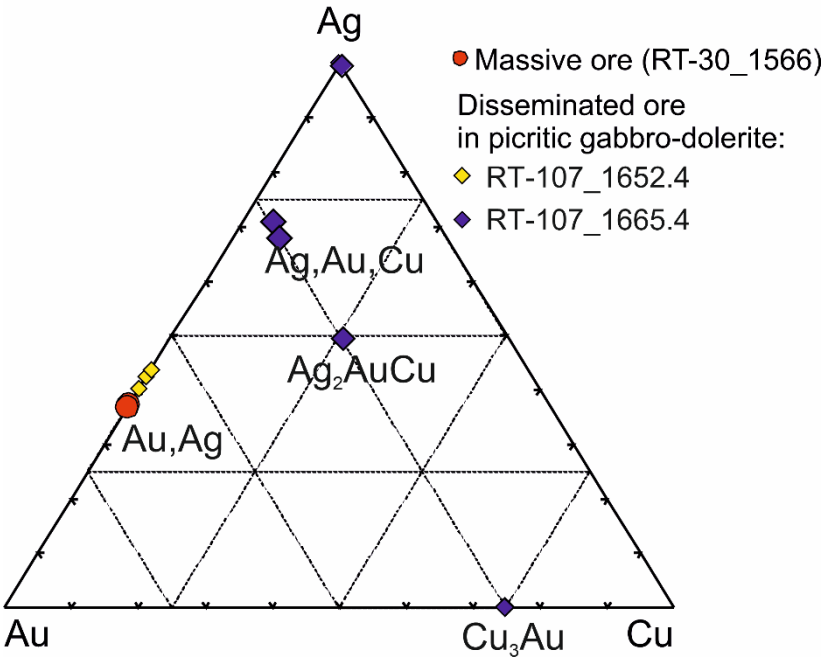

Figure 12.

https://doi.org/10.1180/mgm.2024.20 Published online by Cambridge University Press

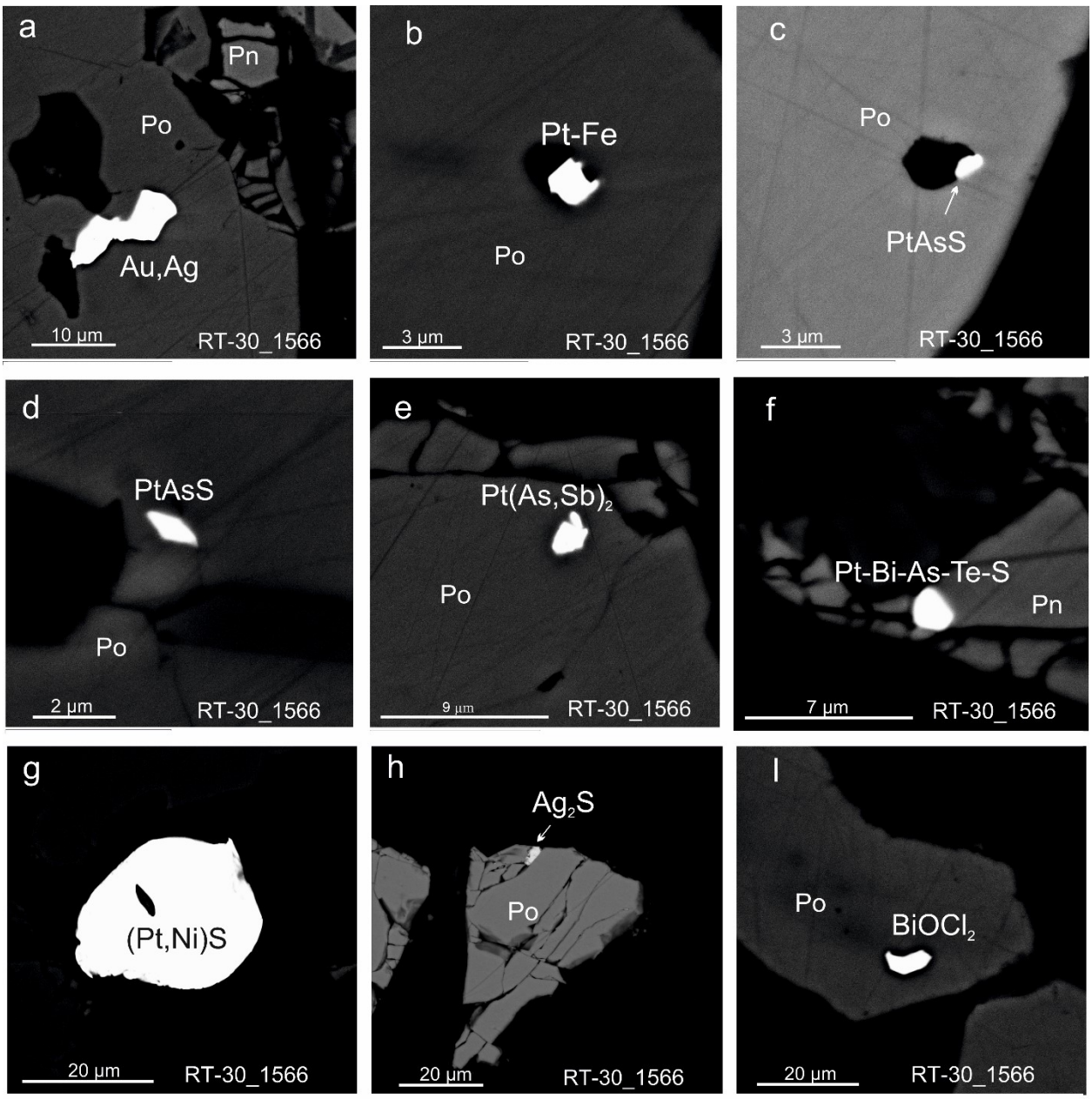

Figure 13.

https://doi.org/10.1180/mgm.2024.20 Published online by Cambridge University Press

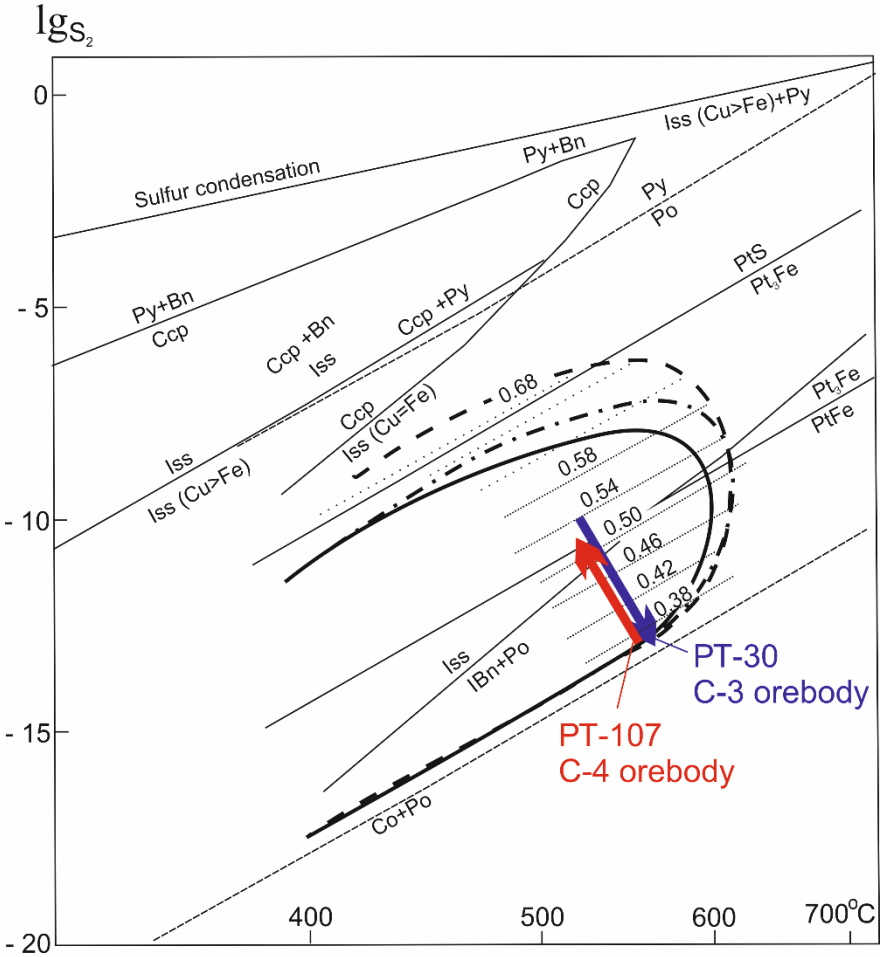

Figure 14.

https://doi.org/10.1180/mgm.2024.20 Published online by Cambridge University Press

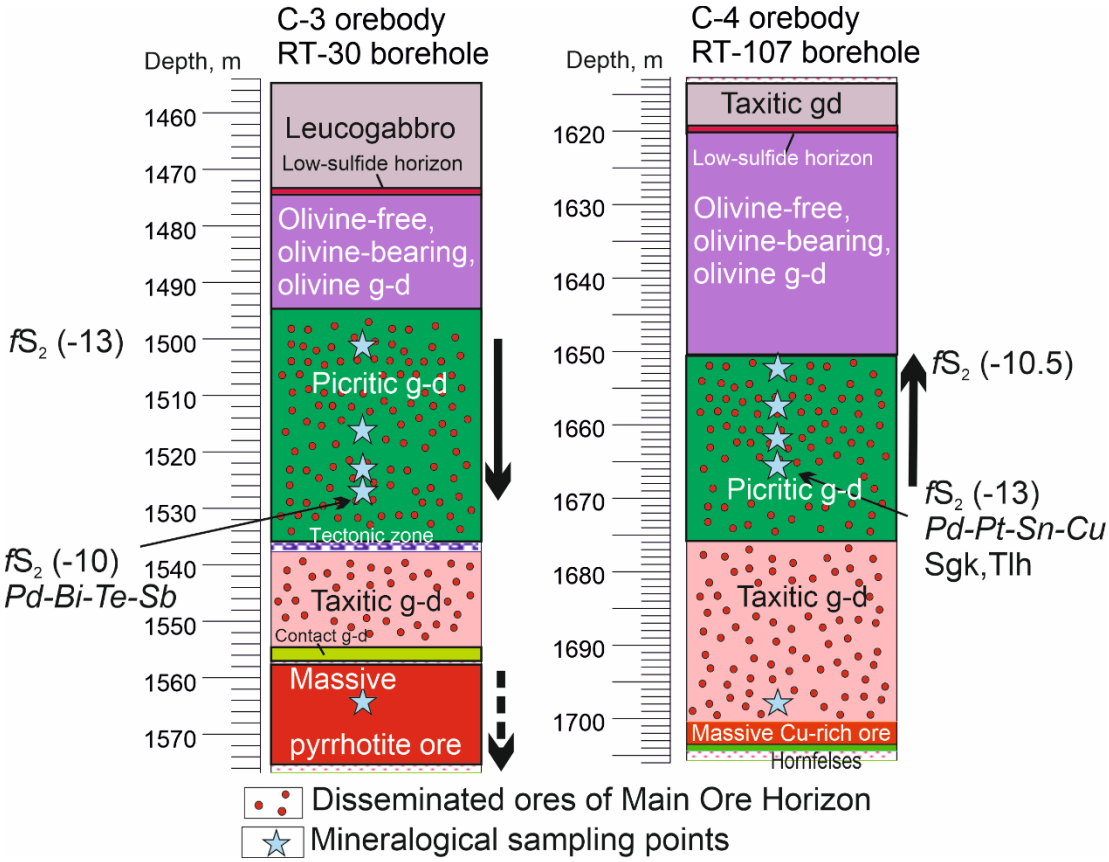

Figure 15.

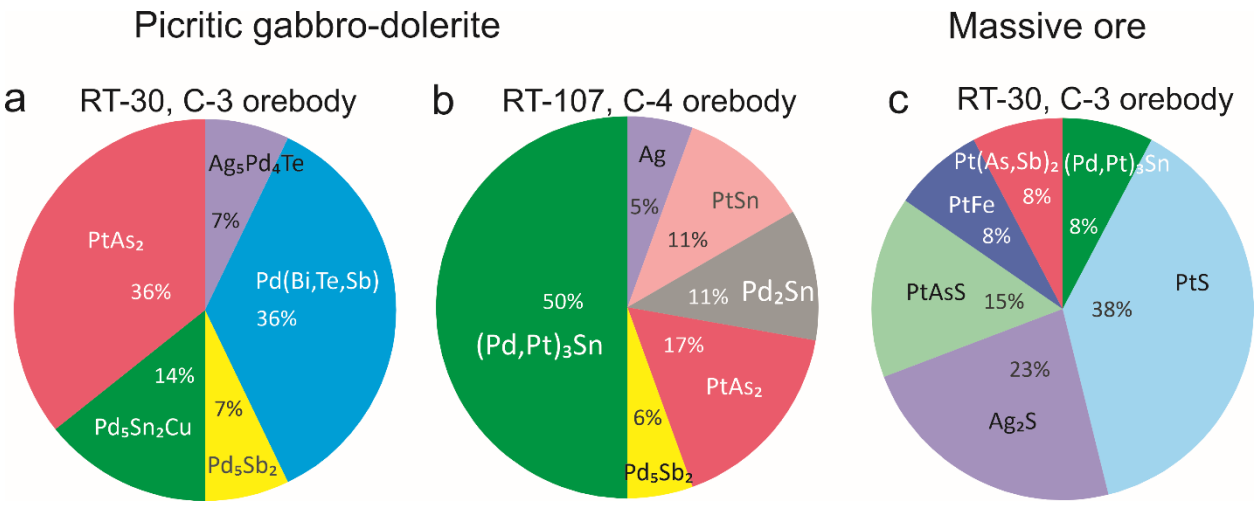

Figure 16

Table 1. Representative compositions of sulfides from boreholes RT-30 and RT-107 of the Oktyabr'sky deposit

No.	Sample, depth	Fe	Co	Ni	Cu	Ag	S	Сумма	Formula
				Disseminated ores in picritic gabbrodolerite					
1	PT-107_1657.2	60.74					38.06	98.8	$Fe_{0.96}S_{1.04}$
2	PT-107_1657.2	60.61					37.71	98.32	$Fe_{0.96}S_{1.04}$

https://doi.org/10.1180/mgm.2024.20 Published online by Cambridge University Press

3	PT-107_1657.2	61.24					37.80	99.04	$Fe_{0.96}S_{1.04}$
4	PT-107_1665.4	58.41		4.01			35.61	99.04	$(Fe_{0.94}Ni_{0.06})_{1.00}S_{1.00}$
5	PT-107_1665.4	57.82	1.44	3.93			36.16	99.35	$(Fe_{0.92}Ni_{0.06}Co_{0.02})_{1.00}S_{1.00}$
6	PT-107_1665.4	58.80		3.88			35.46	99.17	$(Fe_{0.95}Ni_{0.06})_{1.01}S_{0.99}$
7	PT-30_1501.2	63.20					36.25	99.87	$Fe_{1.00}S_{1.00}$
8	PT-30_1501.2	62.80					35.71	99.26	$Fe_{1.00}S_{1.00}$
9	PT-30_1501.2	62.62					35.85	99.17	$Fe_{1.00}S_{1.00}$
10	PT-30_1516	60.68		0.47			37.69	98.84	$(Fe_{0.96}Ni_{0.01})_{0.97}S_{1.04}$
11	PT-30_1516	61.64	0.36	0.34			37.97	100.31	$(Fe_{0.96}Co_{0.01}Ni_{0.01})_{0.98}S_{1.03}$
12	PT-30_1516	61.04					37.36	98.69	$Fe_{0.97}S_{1.03}$
13	PT-30_1523	60.63		0.64			38.48	99.75	$(Fe_{0.95}Ni_{0.01})_{0.96}S_{1.05}$
14	PT-30_1523	60.8		0.63			38.57	100.0	$(Fe_{0.95}Ni_{0.01})_{0.96}S_{1.04}$
15	PT-107_1652	29.24	1.53	36.16			32.83	99.76	$(Ni_{4.78}Fe_{4.07}Co_{0.20})_{9.05}S_{7.95}$
16	PT-107_1652	29.38	1.56	36.12			33.07	100.13	$(Ni_{4.76}Fe_{4.07}Co_{0.20})_{9.03}S_{7.97}$
17	PT-107_1652	29.16	1.43	35.68			32.95	99.22	$(Ni_{4.74}Fe_{4.07}Co_{0.19})_{9.00}S_{8.01}$
18	PT-107_1657.2	35.28	0.69	30.64			33.16	99.77	$(Fe_{4.88}Ni_{4.03}Co_{0.09})_{9.01}S_{7.99}$
19	PT-107_1657.2	35.04	0.80	30.48			33.15	98.67	$(Fe_{4.86}Ni_{4.02}\ Co_{0.11})_{8.99}S_{8.01}$
20	PT-107_1657.2	35.27	0.87	30.32			33.24	98.83	$(Fe_{4.88}Ni_{3.99}\ Co_{0.09})_{8.99}S_{8.01}$
21	PT-107_1665.4	39.54	2.00	24.92			33.17	99.63	$(Fe_{5.47}Ni_{3.28}Co_{0.26})_{9.01}S_{7.99}$
22	PT-107_1665.4	39.5	2.01	25.04			33.08	99.63	$(Fe_{5.47}Ni_{3.30}Co_{0.26})_{9.03}S_{7.97}$
23	PT-107_1665.4	39.16	2.06	25.02			32.65	98.89	$(Fe_{5.47}Ni_{3.32}Co_{0.27})_{9.06}S_{7.94}$
24	PT-107_1665.4	39.20	2.19	25.32			33.11	99.82	$(Fe_{5.42}Ni_{3.33}Co_{0.29})_{9.04}S_{7.97}$
25	PT-107_1665.4	41.70		20.44	3.98		33.32	99.44	$(Fe_{5.78}Ni_{2.69}Cu_{0.48})_{8.95}S_{8.04}$
26	PT-107_1665.4	42.86		16.58	6.89		32.66	98.99	$(Fe_{5.99}Ni_{2.21}Cu_{0.85})_{9.05}S_{7.95}$
27	PT-107_1665.4	43.11		16.16	7.37		32.93	99.57	$(Fe_{5.99}Ni_{2.14}Cu_{0.90})_{9.03}S_{7.97}$
28	PT-107_1665.4	43.38		16.61	6.31		33.08	99.38	$(Fe_{6.03}Ni_{2.20}Cu_{0.77})_{9.00}S_{8.01}$
29	PT-30_1516	32.79	1.84	32.26			32.98	99.87	$(Fe_{5.54}Ni_{4.25}Co_{0.24})_{9.043}S_{7.96}$
30	PT-30_1516	34.07	0.29	31.48			33.05	98.6	$(Fe_{4.75}Ni_{4.18}Co_{0.04})_{8.97}S_{8.03}$
31	PT-30_1516	32.77	3.47	27.99			33.68	97.91	$(Fe_{4.59}Ni_{3.73}Co_{0.46})_{8.78}S_{8.22}$
32	PT-30_1501.2	40.95	0.42	23.73			32.5	97.18	$(Fe_{5.78}Ni_{3.18}Co_{0.06})_{9.02}S_{7.98}$
33	PT-30_1501.2	39.83	0.75	24.81			33.41	98.05	$(Fe_{5.53}Ni_{3.28}\ Co_{0.10})_{8.91}S_{8.09}$
34	PT-30_1501.2	39.58	0.70	24.68			32.98	97.24	$(Fe_{5.55}Ni_{3.29}Co_{0.09})_{8.94}S_{8.06}$
35	PT-30_1523	32.84	1.89	32.88			32.1	97.82	$(Fe_{4.58}Ni_{4.37}Co_{0.25})_{9.20}S_{7.80}$
36	PT-30_1523	31.64	1.13	32.66			33.53	97.83	$(Fe_{4.40}Ni_{4.32}Co_{0.15})_{8.87}S_{8.13}$
37	PT-30_1527	29.52	2.07	34.80			32.94	99.33	$(Ni_{4.62}Fe_{4.11}Co_{0.27})_{9.00}S_{8.00}$
38	PT-30_1527	29.41	1.76	34.70			32.46	98.33	$(Ni_{4.65}Fe_{4.14}Co_{0.24})_{9.03}S_{7.97}$
39	PT-30_1527	32.43	0.48	32.10			32.18	97.19	$(Fe_{4.61}Ni_{4.35}Co_{0.06})_{9.02}S_{7.98}$
40	PT-107_1652	30.34			33.57		34.36	98.27	$Cu_{0.99}Fe_{1.01}S_{2.00}$
41	PT-30_1501.2	33.12			31.51		33.72	98.35	$Cu_{0.93}Fe_{1.11}S_{1.97}$
42	PT-30_1501.2	34.17			29.68		34.55	98.4	$Cu_{0.87}Fe_{1.13}S_{2.00}$
43	PT-30_1516	30.89			33.96		34.46	99.31	$Cu_{0.99}Fe_{1.02}S_{1.99}$
44	PT-30_1516	30.89			33.21		34.3	98.4	$Cu_{0.97}Fe_{1.03}S_{1.99}$
45	PT-30_1523	29.84			33.09		34.34	97.27	$Cu_{0.98}Fe_{1.01}S_{2.02}$
46	PT-30_1523	30.43			33.33		34.24	98.00	$Cu_{0.98}Fe_{1.02}S_{2.00}$
47	PT-107_1665.4	33.05			30.62		34.12	97.79	$Fe_{1.66}Cu_{1.35}S_{2.99}$
48	PT-107_1665.4	32.74			31.12		34.49	98.35	$Fe_{1.66}Cu_{1.30}S_{3.04}$
	Disseminated ores in taxitic gabbro-dolerite								
49	PT-107_1698	61.54					37.94	99.48	$Fe_{0.96}S_{1.04}$
50	PT-107_1698	61.22		0.56			37.92	99.70	$(Fe_{0.96}Ni_{0.01})_{0.97}S_{1.03}$
51	PT-107_1698	60.51					38.59	99.10	$Fe_{0.95}S_{1.05}$
52	PT-107_1698	59.98					38.71	98.69	$Fe_{0.94}S_{1.06}$
53	PT-107_1698	32.62	1.15	33.34			32.85	99.96	$(Fe_{4.52}Ni_{4.40}Co_{0.15})_{9.07}S_{7.93}$
54	PT-107_1698	32.79	1.23	33.26			33.06	100.34	$(Fe_{4.53}Ni_{4.37}Co_{0.16})_{9.06}S_{7.95}$
55	PT-107_1698	37.75		18.90		13.16	31.39	101.20	$Ag_{0.99}(Fe_{5.47}Ni_{2.61})_{8.08}S_{7.93}$
56	PT-107_1698*	33.23		34.25			33.89	101.37	$(Fe_{4.52}Ni_{4.44})_{8.96}S_{8.04}$
57	PT-107_1698*	37.22		18.89		12.92	30.80	99.83	$Ag_{0.98}(Fe_{5.48}Ni_{2.64})_{8.12}S_{7.89}$
58	PT-107_1698	37.22		18.83		12.86	31.03	99.94	$Ag_{0.98}(Fe_{5.46}Ni_{2.63})_{8.09}S_{7.93}$

https://doi.org/10.1180/mgm.2024.20 Published online by Cambridge University Press

59	PT-107_1698	36.05		18.26		13.05	29.97	97.33	$Ag_{1.02}(Fe_{5.45}Ni_{2.63})_{8.08}S_{7.90}$
60	PT-107_1698	35.95		24.61		7.50	31.93	99.99	$(Fe_{5.14}Ni_{3.65}Ag_{0.56})_{9.05}S_{7.95}$
61	PT-107_1698	33.16	0.98	22.46		5.64	37.19	99.43	$(Fe_{4.58}Ni_{2.95}Ag_{0.40}Co_{0.13})_{8.06}S_{8.}$
62	PT-107_1698	31.08			34.37		34.35	99.80	$Cu_{1.00}Fe_{1.03}S_{1.98}$
63	PT-107_1698*	30.93			34.26		34.26	99.45	$Cu_{1.00}Fe_{1.02}S_{1.98}$
64	PT-107_1698	30.93			34.26		34.26	99.45	$Cu_{1.00}Fe_{1.02}S_{1.98}$
65	PT-107_1698	35.08	0.11		30.10		35.08	100.37	$Cu_{1.29}(Fe_{1.71}Co_{0.01})_{1.72}S_{2.99}$
66	PT-107_1698	35.72	0.09	0.10	29.65		34.55	100.11	$Fe_{1.75}Cu_{1.28}S_{2.96}$
					Massive ore				
67	PT-30_1566	60.50		0.48			38.13	99.11	$(Fe_{0.95}Ni_{0.01})_{0.96}S_{1.04}$
68	PT-30_1566	60.75		0.56			38.75	100.06	$(Fe_{0.94}Ni_{0.01})_{0.95}S_{1.05}$
69	PT-30_1566	60.36		0.57			38.71	99.64	$(Fe_{0.94}Ni_{0.01})_{0.95}S_{1.05}$
70	PT-30_1566	60.51		0.60			37.59	98.70	$(Fe_{0.96}Ni_{0.01})_{0.97}S_{1.03}$
71	PT-30_1566	33.13	1.42	31.48			33.59	99.62	$(Fe_{4.58}Ni_{4.14}Co_{0.19})_{8.91}S_{8.09}$
72	PT-30_1566	32.32	1.54	31.82			32.86	98.54	$(Fe_{4.53}Ni_{4.24}Co_{0.20})_{8.97}S_{8.02}$
73	PT-30_1566	31.40	1.65	33.63			33.08	99.76	$(Ni_{4.44}Fe_{4.35}Co_{0.22})_{9.01}S_{7.99}$
74	PT-30_1566	30.68	1.78	33.69			33.20	99.35	$(Ni_{4.46}Fe_{4.27}Co_{0.23})_{8.96}S_{8.04}$
75	PT-30_1566	30.81	1.66	34.25			33.09	99.81	$(Ni_{4.52}Fe_{4.27}Co_{0.22})_{9.01}S_{7.99}$
76	PT-30_1566	29.87			33.14		34.92	97.93	$Cu_{0.97}Fe_{1.00}S_{2.03}$
77	PT-30_1566	38.45			25.44		35.16	99.05	$Fe_{1.89}Cu_{1.10}S_{3.01}$

The table presents the sample compositions of sulfides and it is built on the principle of changing their compositions with depth from the upper parts of the picrite layers to the lower ones for each borehole.

1-14, 49-52, 67-70 – pyrrhotite (Fe,Ni,Co)S; 15-24, 29-39, 53-61, 71-75 – pentlandite $(Fe,Ni)_9S_8$; 25-28 – sugakiite $Cu(Fe,Ni)_8S_8$; 40-46, 62-65, 76 – chalcopyrite $CuFeS_2$; 47-48, 65-66, 77 – cubanite Fe_2CuS_3; Sample PT-107*1698* - Compositions shown in Figure 7.

https://doi.org/10.1180/mgm.2024.20 Published online by Cambridge University Press

Table 2. Compositions of PGM, wt %

No.	Sample	Ni	Pt	Pd	Cu	Au	Sn	Sb	Te	As	Bi	S	Total	Formula
							Disseminated ores in picritic gabbrodolerite							
1	PT-30_1501.2		55.81							42.75			98.56	$Pt_{1.00}As_{2.00}$
2	PT-30_1501.2		55.65							42.36			98.01	$Pt_{0.98}As_{2.02}$
3	PT-30_1527		54.72							43.37			98.09	$Pt_{0.98}As_{2.02}$
4	PT-107_1657.2		55.61							41.56			97.17	$Pt_{1.02}As_{1.98}$
5	PT-107_1665.4		56.33							41.78			98.11	$Pt_{1.02}As_{1.98}$
6	PT-107_1665.4		55.64							41.94			97.58	$Pt_{1.01}As_{1.99}$
7	PT-30_1516			36.99					19.43		42.1		98.53	$Pd_{0.99}(Bi_{0.57}Te_{0.44})_{1.01}$
8	PT-30_1516			36.73					19.14		42.0		97.90	$Pd_{0.99}(Bi_{0.58}Te_{0.43})_{1.01}$
9	PT-30_1527			36.25				2.08	11.88		48.1		98.36	$Pd_{1.00}(Bi_{0.68}Te_{0.27}Sb_{0.05})_{1.00}$
10	PT-30_1527			36.37				2.25	11.97		46.7		97.35	$Pd_{1.01}(Bi_{0.66}Te_{0.28}Sb_{0.05})_{0.99}$
11	PT-30_1527			36.57				1.71	21.64		38.2		98.21	$Pd_{0.97}(Bi_{0.52}Te_{0.48}Sb_{0.04})_{1.04}$
12	PT-30_1527			36.87				3.99	17.26		39.9		98.07	$Pd_{0.98}(Bi_{0.54}Te_{0.38}Sb_{0.09})_{1.01}$
13	PT-30_1527			66.70				31.12					97.82	$Pd_{4.97}Sb_{2.03}$
14	PT-107_1652		60.00				37.65						97.65	$Pt_{0.98}Sn_{1.02}$
15	PT-107_1652		60.01				37.39						97.40	$Pt_{0.99}Sn_{1.01}$
16	PT-107_1665.4		5.25	59.46			34.53						99.24	$(Pd_{1.91}Pt_{0.09})_{2.00}Sn_{1.00}$
17	PT-107_1665.4		3.49	61.00			35.06						99.55	$(Pd_{1.94}Pt_{0.06})_{2.00}Sn_{1.00}$
18	PT-107_1665.4		2.86	61.44			32.92	3.41					100.63	$(Pd_{1.93}Pt_{0.05})_{1.98}(Sn_{0.93}Sb_{0.09})_{1.02}$
19	PT-30-1527		12.01	53.64	7.52		25.64	2.01					100.82	$(Pd_{4.40}Pt_{0.54})_{4.94}(Sn_{1.89}Sb_{0.14})_{2.03}Cu_{1.03}$
20	PT-30-1527		10.98	53.58	7.42		25.90						97.88	$(Pd_{4.50}Pt_{0.50})_{5.00}Sn_{1.95}Cu_{1.04}$
21	PT-107_1652		57.89	16.61		4.9	19.57						98.97	$(Pt_{1.85}Pd_{0.97}Au_{0.15})_{2.97}Sn_{1.03}$
22	PT-107_1665.4		21.85	46.43	0.36	5.77	23.47						97.88	$(Pd_{2.23}Pt_{0.57}Au_{0.15}Cu_{0.03})_{2.98}Sn_{1.01}$
23	PT-107_1665.4		35.73	36.57	0.53	2.51	21.43	1.24					98.01	$(Pd_{1.86}Pt_{0.99}Au_{0.07}Cu_{0.05})_{2.97}(Sn_{0.98}Sb_{0.06})_{1.0}$
24	PT-107_1665.4		39.30	34.09	0.69	2.55	21.15						97.78	$(Pd_{1.77}Pt_{1.11}Au_{0.07}Cu_{0.06})_{3.01}Sn_{0.98}$
25	PT-107_1665.4		45.66	29.12	0.46	2.05	20.81	1.27					99.37	$(Pd_{1.54}Pt_{1.32}Au_{0.06}Cu_{0.04})_{2.96}(Sn_{0.99}Sb_{0.06})_{1.0}$
26	PT-107_1665.4		63.27	15.72	0.39		18.87						98.25	$(Pt_{2.04}Pd_{0.93}Cu_{0.04})_{3.01}Sn_{1.00}$

https://doi.org/10.1180/mgm.2024.20 Published online by Cambridge University Press

27	PT-107_1665.4		10.11	46.39	13.2	27.54			97.19	$(Pd_{1.88}Cu_{0.89}Pt_{0.22})_{2.99}Sn_{1.00}$
28	PT-107_1665.4		4.18	51.5	13.3	28.2			97.18	$(Pd_{2.03}Cu_{0.88}Pt_{0.09})_{3.00}Sn_{1.00}$
						Disseminated ores in taxitic gabbrodolerite				
29	PT-107бис_1695			65.68		23.58	8.26		97.52	$Pd_{2.00}(Sn_{0.64}As_{0.36})_{1.00})$
30	PT-107бис_1695			62.09		34.77			96.86	$Pd_{2.00}Sn_{1.00}$
						Massive ore				
31	PT-30_1566	0.84	83.04	1.06				14.69	99.63	$(Pt_{0.94}Ni_{0.03}Pd_{0.02})_{0.99}S_{1.01}$
32	PT-30_1566	0.71	82.94	0.77				14.57	98.99	$(Pt_{0.95}Ni_{0.03}Pd_{0.02})_{1.00}S_{1.00}$
33	PT-30_1566	0.79	83.05	0.70				14.78	99.32	$(Pt_{0.94}Ni_{0.03}Pd_{0.01})_{0.98}S_{1.02}$
34	PT-30_1566	0.90	81.03	0.90				14.65	97.48	$(Pt_{0.93}Ni_{0.03}Pd_{0.02})_{0.98}S_{1.02}$
35	PT-30_1566	0.52	84.60					15.02	100.14	$(Pt_{0.95}Ni_{0.02})_{0.97}S_{1.03}$

* – the total of the mineral analysis after subtracting the composition of the sulfide matrix; 1-6 – sperrylite $PtAs_2$; 7-12 – sobolevskite Pd(Bi,Te,Sb); 13 – stibiopalladinite Pd_5Sb_2; 14, 15 – niggliite PtSn; 16-18, 29-30 – paolovite $Pd_2(Sn,As,Sb)$; 19-20 – stannopalladinite Pd_5Sn_2Cu; 21-26 - rustenburgite-atokite solid solutions $(Pd,Pt,Cu)_3Sn$; 27-28 – taimirite-cabriite solid solution $(Pd,Pt,Cu)_3Sn$; 31-35 – cooperite PtS.

https://doi.org/10.1180/mgm.2024.20 Published online by Cambridge University Press

Table 3. Compositions of Au-Ag alloys from the Oktyabr'sky deposit

No.	Sample_depth	Au	Ag	Cu	Total	Au	Ag	Cu	Total
		Wt.%				At.%			
Disseminated ores in picritic gabbrodolerites (Orebody C-4)									
3	PT-107_1665.4		98.48		98.48		100.0		100.0
4	PT-107_1665.4		99.82		99.82		100.0		100.0
5	PT-107_1665.4	49.91		47.89	97.8	25.16	0.00	74.84	100.0
6	PT-107_1665.4	49.18		47.15	96.33	25.18	0.00	74.82	100.0
7	PT-107_1665.4	39.98	43.93	14.21	98.12	24.34	48.84	26.82	100.0
8	PT-107_1665.4	39.26	59.92	2.13	101.31	25.28	70.46	4.25	100.0
9	PT-107_1665.4	40.03	58.82	2.96	101.81	25.56	68.58	5.86	100.0
Massive ore (Orebody C-3)									
1	PT-30_1566	71.25	23.17		94.42	62.74	37.26		100.0
2	PT-30_1566	70.5	22.36		92.86	63.33	36.67		100.0

https://doi.org/10.1180/mgm.2024.20 Published online by Cambridge University Press